Am J Transl Res 2017;9(8):3558-3572
www.ajtr.org /ISSN:1943-8141/AJTR0050789

Original Article

A proteomics-based investigation on the anticancer activity of alisertib, an Aurora kinase A inhibitor, in hepatocellular carcinoma Hep3B cells

Qiaohua Zhu[1,2], Meihua Luo[1], Chengyu Zhou[1], Zhiwei Zhou[2], Zhixu He[3], Xinfa Yu[1], Shufeng Zhou[2,4]

[1]Department of Oncology and Interventional Radiology, Shunde Hospital, Southern Medical University, Shunde 528300, Guangdong, China; [2]Department of Pharmaceutical Sciences, College of Pharmacy, University of South Florida, Tampa, FL, USA; [3]Guizhou Provincial Key Laboratory for Regenerative Medicine, Stem Cell and Tissue Engineering Research Center & Sino-US Joint Laboratory for Medical Sciences, Guiyang Medical University, Guiyang 550004, China; [4]Department of Bioengineering and Biotechnology, College of Chemical Engineering, Huaqiao University, Xiamen 361021, Fujian, China

Received November 10, 2016; Accepted June 16, 2017; Epub August 15, 2017; Published August 30, 2017

Abstract: Targeted therapy may provide survival benefit for advanced hepatocellular carcinoma (HCC) and Aurora A kinase (AURKA) represents a feasible target in cancer treatment. The purpose of this study is to investigate the anticancer activity of alisertib (ALS) on Hep3B cells based on a proteomic study conducted with the stable-isotope labeling by amino acids in cell culture (SILAC). The proteomic response to ALS was obtained with SILAC-based proteomic study. Cell cycle distribution and apoptosis were assessed using flow cytometry and autophagy was determined using flow cytometry and confocal microscopy. ALS inhibited the proliferation of Hep3B cells, with IC_{50} values for 24- and 48-h exposure of 46.8 and 28.0 μM, respectively. Our SILAC study demonstrated that there were at least 565 proteins responding to ALS treatment, with 256 upregulated, 275 downregulated and 35 stable. Ninety-four signaling pathways, majority of which involved cell proliferation and survival, programmed cell death, and nutrition and energy metabolism, were regulated by ALS. ALS significantly inhibited the phosphorylation of AURKA at Thr288 in a concentration-dependent manner. Subsequent study showed that ALS remarkably arrested Hep3B cells in G_2/M phase via regulating the expression of key cell cycle regulators, and induced a marked autophagy via the PI3K/Akt/mTOR axis. Inhibition of autophagy enhanced the anticancer activity of ALS in Hep3B cells. Overall, ALS leads to comprehensive proteomic response, inhibits cellular proliferation, and induces cell cycle arrest and autophagy in Hep3B cells. Further studies are warranted to explore the role of ALS in the treatment of HCC.

Keywords: Hepatocellular carcinoma, Hep3B cells, Aurora kinase A, alisertib, cell cycle, apoptosis, autophagy, SILAC, proteomics

Introduction

Liver cancer is the sixth most common cancer and the second leading cause of cancer-related death worldwide despite the development of various screening, preventive and therapeutic strategies [1]. It is the fifth most common cancer in men (554,000 cases, 7.5% of the total) and the ninth in women (228,000 cases, 3.4%). According to the GLOBOCAN 2012, an estimated 782,500 new liver cancer cases accounting for 5.6% of all cancers diagnosed and 745,500 deaths (9.1% of total) occurred worldwide during 2012 [1]. Hepatocellular carcinoma (HCC) accounts for 85-90% of all liver cancer [2, 3]. Currently, surgical therapy including resection and transplantation remains the curative treatment options for HCC, however, only a small portion of the patients with HCC are candidates for surgery due to delayed diagnosis [4-8]. The 1-year survival rate for people with liver cancer is 44% and the 5-year survival rate is 17% [2, 3]. The median overall survival of the patients with advanced HCC is less than one year and the 5-year survival rate is less than 10%. In recently years, a number of studies have demonstrated that systemic treatment options, such as molecular target therapy and systemic chemo-

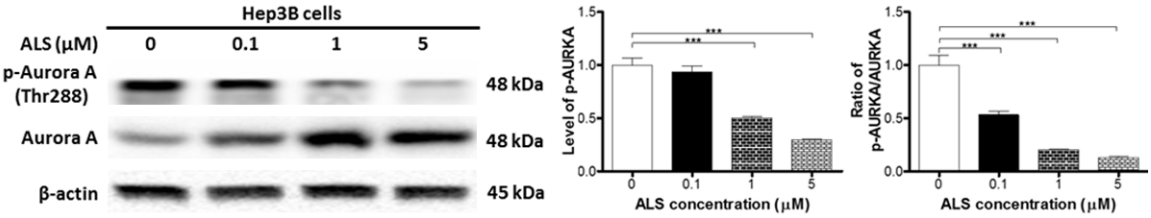

Figure 1. ALS inhibits the phosphorylation of AURKA in Hep3B cells. Hep3B cells were incubated with ALS at 0.1, 1, and 5 μM for 24 h, and the protein samples were subject to Western blotting assay. Representative blots of p-AURKA and AURKA. Bar graphs show the relative level of p-AURKA and ratio of p-AURKA/AURKA. β-Actin was used as the internal control. Data are the mean ± SD of three independent experiments. ***$P < 0.001$ by one-way ANOVA.

therapy, were able to provide definite survival benefit for late-stage HCC patients [5, 8-14]. So far, sorafenib, an oral multitargeted tyrosine kinase inhibitor, is still the standard treatment for advanced HCC, although a series of clinical studies on new targeted agents for HCC have been completed or still ongoing [7-9, 14, 15].

Aurora kinases, which play an important role in regulating mitosis, cell division, and cell cycle progression, are comprised of three family members, including Aurora kinase A (AURKA), AURKB, and AURKC [16, 17]. AURKA is essential for the timely entry into the M phase of the cell cycle, maintaining spindle bipolarity and chromosome segregation, while AURKB is required for chromosome condensation, alignment on the spindle, spindle checkpoint function, and cytokinesis. The knowledge of AURKC function is limited [18]. Aberration in the activity of AURKA lead to improper mitotic progression and has been implicated in the pathogenesis of various cancers [16, 17]. Overexpression and amplification of AURKA in HCC have been associated with aggressive tumor characteristics, chemoresistance and poor prognosis in HCC [19-21]. These findings indicate AURKA could be a potential target for the treatment of HCC.

Alisertib (ALS, MLN8237, see Figure S1), an investigational small-molecule inhibitor, selectively inhibits AURKA [22]. Studies by us and other groups have demonstrated the anticancer effect of ALS on various types of cancers in preclinical models [23-32]. Besides, a number of Phase I and Phase II clinical trials investigating the effect of ALS for advanced solid tumors and hematologic malignancies have been completed or are ongoing, and have shown some promising results [22]. However, the evidence of the effect of ALS on HCC is very limited. In the present study, the anticancer activity of ALS in HCC Hep3B cells, such as anti-proliferation, inducing effect on cell cycle arrest and programmed cell death, was investigated based on a proteomic study conducted with the method of stable-isotope labeling by amino acids in cell culture (SILAC).

Materials and methods

Chemicals and reagents

ALS, MK-2206 and rapamycin were purchased from Selleckchem Inc. (Houston, TX, USA). Wortmannin (a PI3K inhibitor and a blocker of autophagosome formation) were purchased from Invivogen Inc. (San Diego, CA, USA). Dulbecco's phosphate buffered saline (PBS), fetal bovine serum (FBS), thiazolyl blue tetrazolium bromide (MTT), RNase A, dimethyl sulfoxide (DMSO), 7-amino-actinomycin D (7-AAD), propidium iodide (PI), $^{13}C_6$ L-lysine, $^{13}C_6$ $^{15}N_4$ L-arginine and L-arginine, and chloroquine (CQ) were purchased from Sigma-Aldrich Inc. (St Louis, MO, USA). Dulbecco's Modified Eagle's Medium (DMEM) were obtained from Corning Cellgro Inc. (Herndon, VA, USA). Phenol red-free culture medium and 4,6-diamidino-2-phenylindole were bought from Invitrogen (Carlsbad, CA, USA). The annexinV: phycoerythrinv (PE) apoptosis detection kit was purchased from BD Biosciences Inc. (San Jose, CA, USA). The Cyto-ID® autophagy detection kit was obtained from Enzo Life Sciences Inc. (Farmingdale, NY, USA). The Pierce bicinchoninic acid (BCA) protein assay kit, skim milk, and western blot substrate were purchased from Thermo Scientific (Waltham, MA, USA). Polyvinylidene difluoride (PVDF) membrane was purchased from EMD Millipore (Bedford, MA, USA). Primary antibodies against human cyclin B1, p-cyclin B1 at Ser 133, cell division cycle protein 2 homologue

(CDC2), p-CDC2 at Tyr15, phosphorylated (p)-CDC25C at Ser216, Akt, p-Akt at Ser473, mammalian target of rapamycin (mTOR), p-mTOR at Ser2448, PI3K, p-PI3K at Tyr458, AURKA, p-AURKA at Thr288, phosphatase and tensin homolog (PTEN), beclin1, SQSTM1/p62, microtubule-associated protein 1A/1B-light chain 3 (LC3)-I, and LC3-II were all purchased from Cell Signaling Technology Inc. (Beverly, MA, USA). The antibody against human β-actin was obtained from Santa Cruz Biotechnology Inc. (Santa Cruz, CA, USA).

Cell lines and cell culture

Hep3B cell line was obtained from the American Type Culture Collection (Manassas, VA, USA) and cultured in DMEM medium supplemented with 10% heat-inactivated FBS and 1% penicillin/streptomycin. The cells were maintained in a 5% CO_2/95% air-humidified incubator at 37°C. ALS was dissolved in DMSO with a stock concentration of 50 mM and the stock solution was stored at -20°C. ALS was freshly diluted to the predetermined concentrations with culture medium. The final concentration of DMSO was at 0.05% (v/v). The control cells received the vehicle only.

Quantitative proteomic study using SILAC

Quantitative proteomic experiments were performed using a SILAC-based approach as described previously [31, 33-38]. Briefly, Hep3B cells were cultured in DMEM-F12 medium (for SILAC) with (heavy) or without (light) stable isotope labeled amino acids ($^{13}C_6$ L-lysine and $^{13}C_6$ $^{15}N_4$ L-arginine) and 10% dialyzed FBS. Hep3B cells cultured in heavy medium were treated with 1 μM ALS for 24 h after six cell doubling times. After treatment with ALS, Hep3B cells were harvested and lysed with hot lysis buffer [100 mM Tris base, 4% sodium dodecyl sulfate (SDS), and 100 mM dithiothreitol], and protein concentration was determined using ionic detergent compatibility reagent. Subsequently, equal amounts of heavy and light protein samples were combined to reach a total volume of 30-60 μL containing 300-600 μg protein. The combined protein sample was digested using a filter-aided sample prep (FASP™) protein digestion kit and desalted using a C_{18} solid-phase extraction column. The peptide mixtures (5 μL) were subject to the hybrid linear ion trap (LTQ Orbitrap XL™, Thermo Fisher Scientific Inc.). Liquid chromatography-tandem mass spectrometry was performed using a 10-cm long, 75 μm (inner diameter) reversed-phase column packed with 5 μm diameter C_{18} material having a pore size of 300 Å (New Objective Inc., Woburn, MA, USA) with a gradient mobile phase of 2%-40% acetonitrile in 0.1% formic acid at 200 μL per min for 125 min. The Orbitrap full mass spectrometry scanning was performed at a mass (m/z) resolving power of 60,000, with positive polarity in profile mode ($M+H^+$). Peptide SILAC ratio was calculated using MaxQuant version 1.2.0.13. The SILAC ratio was determined by averaging all peptide SILAC ratios from peptides identified of the same protein. The protein IDs were identified using Scaffold 4.3.2 from Proteome Software Inc. (Portland, OR, USA).

Cell viability assay

The MTT assay was performed to examine the effect of ALS on cell viability. Briefly, Hep3B cells were seeded in 96-well culture plates at a density of 8,000 cells per well. After incubation for 24 h, the cells were treated with ALS at different concentrations ranging from 0.1 to 100 μM for 24 or 48 h. Cell viability was determined by the MTT assay. Absorbance at the 450 nm wavelength was measured with a Synergy H4 Hybrid microplate reader (BioTek Inc., Winooski, VT, USA). IC_{50} values were determined using the relative viability over ALS concentration curve.

Cell cycle distribution analysis

The effect of ALS on cell-cycle distribution of Hep3B cells was examined using flow cytometry. Hep3B cells were treated with ALS at 0.1, 1, and 5 μM for 24 h, or treated with 1 μM ALS for 4, 8, 12, 24, 36 and 60 h. After treatment with ALS, cells were trypsinized, collected, and fixed in 70% ethanol at -20°C for 24 h. Following the fixation, cells were centrifuged and resuspended in 1 mL of PBS containing 1 mg/mL RNase A and 50 μg/mL PI, and incubated in the dark for 30 min at room temperature. A total number of 1×10^4 cells were subject to cell-cycle analysis using a flow cytometer (Becton Dickinson Immunocytometry Systems, San Jose, CA, USA).

Quantification of cellular apoptosis

Hep3B cells were treated with ALS at 0.1, 1, and 5 μM for 24 h, or treated with 1 μM ALS for 4, 8, 12, 24, 36 and 60 h, then subject to flow

Table 1. The top 10 IPA canonical pathways regulated by alisertib in Hep3B cells

Ingenuity canonical pathways	*P*-value	Ratio (H/L)
EIF2 signaling	1.4×10^{-33}	48/185 (0.259)
Regulation of eIF4 and p70S6K signaling	2.67×10^{-17}	29/146 (0.199)
Remodeling of epithelial adherens junctions	4.42×10^{-17}	21/68 (0.309)
RAN signaling	3.08×10^{-12}	10/17 (0.588)
mTOR signaling	8.62×10^{-12}	26/188 (0.138)
Protein ubiquitination pathway	6.9×10^{-11}	29/255 (0.114)
Epithelial adherens junction signaling	4.07×10^{-10}	21/146 (0.144)
tRNA charging	4.2×10^{-9}	11/39 (0.282)
Glycolysis I	9.83×10^{-9}	9/25 (0.36)
Gluconeogenesis I	9.83×10^{-9}	9/25 (0.36)

Abbreviations: EIF, eukaryotic initiation factor; H, medium supplemented with stable isotope-labeled l-arginine and l-lysine; L, medium supplemented with normal l-arginine and l-lysine; mTOR, mammalian target of rapamycin.

Table 2. Top five molecular and cellular functions regulated by alisertib in Hep3B cells

Names	*P*-value range	Number of molecules
Cellular growth and proliferation	5.45×10^{-4}-5.84×10^{-33}	271
Protein synthesis	6.12×10^{-4}-2.27×10^{-30}	140
Cell death and survival	6.24×10^{-4}-3.81×10^{-30}	264
RNA posttranscriptional modification	4.13×10^{-4}-2.38×10^{-20}	53
Gene expression	1.41×10^{-4}-1.58×10^{-19}	153

cytometric analysis. The effect of ALS on the apoptosis of Hep3B cells was quantitated using the annexin V: PE apoptosis detection kit (BD Biosciences Inc.) according to the manufacturer's instruction.

Quantification of cellular autophagy

Hep3B cells were treated with ALS at 0.1, 1, and 5 μM for 24 h, or treated with 1 μM ALS for 4, 8, 12, 24, 36 and 60 h, then subject to flow cytometry for analyzing the intracellular autophagy level. The cells were dyed with green detection and Hoechst 33342 nuclear stain reagent contained in the Cyto-ID® autophagy detection kit (No. ENZ-51031-K200) according to the manufacturer's instructions. The cells were analyzed using the green (FL1) channel of a flow cytometer (Becton Dickinson Immunocytometry Systems).

Confocal fluorescence microscopy examination

Hep3B cells were treated with ALS at 0.1, 1, and 5 μM for 24 h, then subjected to confocal fluorescence microscopy for detecting the intracellular autophagy level. The cells were processed with the Cyto-ID® autophagy detection kit (No. ENZ-51031-K200) according to the manufacturer's instructions. The cells were examined using a Leica TCS SP2 laser scanning confocal microscopy (Leica Microsystems, Wetzlar, Germany) using a standard FITC filter set for imaging the autophagic signal at wavelengths of 405/488 nm.

Western blotting analysis

Hep3B cells were treated with ALS at 0.1, 1, and 5 μM for 24 h and the protein samples were subject to western blotting assay to determine the expression levels of various cellular proteins. Visualization was performed using Bio-Rad ChemiDoc™ XRS system (Hercules, CA, USA) with enhanced chemiluminescence substrate. The blots were analyzed using Image J and protein level was normalized to the matching densitometric value of β-actin as internal control.

Statistical analysis

Data are presented as mean ± standard deviation (SD). Comparisons of multiple groups were evaluated by one-way analysis of variance followed (ANOVA) by Tukey's multiple comparison procedure. A value of $P < 0.05$ was considered statistically different. Assays were performed at least three times independently.

Results

ALS inhibits the proliferation of Hep3B cells

We first examined the effect of ALS on the proliferation of Hep3B cells using the MTT assay. The results showed that ALS treatment inhibited the proliferation of Hep3B cells in a concentration-and time-dependent manner. Compared to the control cells (100%), the viability of Hep3B cells decreased to 89.0%, 85.5%, 82.0%, 63.2%, 49.9% and 36.5%, respectively,

when cells were treated with ALS at 0.1, 1, 5, 25, 50 and 100 μM, respectively, for 24 h. After incubation for 48 h, the viability decreased to 99.8%, 96.7%, 87.2%, 58.4%, 35.5% and 12.6%, respectively (Figure S1). The IC_{50} values for 24 and 48-h ALS treatment were 46.8 and 28.0 μM, respectively.

Proteomic response to ALS treatment in Hep3B cells

To investigate the molecular targets of ALS in Hep3B cells, we next performed a SILAC-based proteomic study with ALS. Our results revealed that 565 protein molecules in all had been identified as potential molecular targets of ALS in Hep3B cells, with 256 protein molecules being upregulated, 275 protein molecules being downregulated and 35 protein molecules stable (Table S1). Then these identified proteins were subject to IPA analysis. The IPA results showed that 94 signaling pathways were regulated by ALS in Hep3B cells (Table S2 and Figure S2), with EIF2 signaling, regulation of eIF4 and p70S6K signaling, remodeling of epithelial adherens junctions, RAN signaling, mTOR signaling, protein ubiquitination pathway, epithelial adherens junction signaling, tRNA charging, glycolysis I, and gluconeogenesis I as the top ten pathways (**Table 1**). More than one fourth of them were involved in the nutrition and energy metabolism. Cellular growth and proliferation, protein synthesis, cell death and survival, RNA post-transcriptional modification and gene expression have been identified as the top five molecular and cellular functions regulated by ALS in Hep3B cells (**Table 2**). ALS regulated cell cycle at G_2/M checkpoint in Hep3B cells (Figure S3). The mTOR signaling pathway was also regulated by ALS in Hep3B cells (Figure S4). Taken together, IPA analysis results have showed the proteins regulated by ALS are involved in a number of important cellular processes, in particular, cell proliferation and survival, programmed cell death, and nutrition and energy metabolism (intracellular hemostasis). Then we focus on analyzing the effect of ALS on the proliferation, cell cycle distribution, apoptosis and autophagy.

ALS inhibits the phosphorylation of AURKA in Hep3B cells

To verify the proteomic data from the SILAC assay, we conducted a series of cell-based functional assays. We first examined its effect on the phosphorylation of the present kinase in Hep3B cells. As shown in **Figure 1**, ALS treatment significantly inhibited the phosphorylation of AURKA at Thr288 in a concentration-dependent manner. Compared to the control cells, a reduction of 49.7% and 70.3% of the p-AURKA level was detected when Hep3B cells were treated with ALS at 1 and 5 μM, respectively, for 24 h ($P < 0.05$ or 0.001). Accordingly, the ratio p-AURKA over AURKA decreased by 79.5% and 86.9%, respectively ($P < 0.001$). These results demonstrate ALS exerts its effect on Hep3B cells via inhibiting the phosphorylation of AURKA.

ALS leads to G_2/M phase arrest and accumulation of aneuploidy in Hep3B cells

Since AURKA is a cell cycle-regulatory kinase and IPA analysis revealed that ALS had a remarkable role in the regulation of G_2/M DNA damage checkpoint (Table S2 and Figure S3), we next examined the effect of ALS on the cell cycle distribution of Hep3B cells using flow cytometry. Our results showed that ALS treatment arrested Hep3B cells at G_2/M phase and induced accumulation of aneuploidy in a concentration- and time-dependent manner (**Figure 2**). The percentage of Hep3B cells arrested in G_2/M phase ascended to 29.3%, 84.6% and 73.1% when treated with ALS at 0.1, 1 and 5 μM for 24 h, respectively, compared to the control cells (with a basal level of 14.4%) (**Figure 2A**).

The effect of ALS treatment at 1 μM on cell cycle distribution in Hep3B cells over 60 h were further evaluated (**Figure 2B**). After exposed to ALS for 4, 8, 12, 24, 36 and 60 h, the percentage of Hep3B cells in G_2/M phase increased to 37.4%, 47.1%, 59.6%, 89.7%, 95.4% and 94.4%, respectively, from the basal level 29.9%. Of note, prolonged ALS treatment over 36 h led to accumulation of aneuploid cells. The percentage of diploid and aneuploid cells at 36 h and 60 h after ALS treatment were 17.4% and 82.6%, and 20.8% and 79.2%, respectively. In the population of aneuploid cells, the percentage of cells arrested in G_2/M phase increased to 34.7% at 60 h from 11.9% at 36 h. A significant reduction of cells in both G_1 and S phase was observed in a concentration- and time-dependent manner (**Figure 2**). Taken together, these results demonstrate that ALS alters the cell cycle distribution of Hep3B cells and induces G_2/M phase arrest and accu-

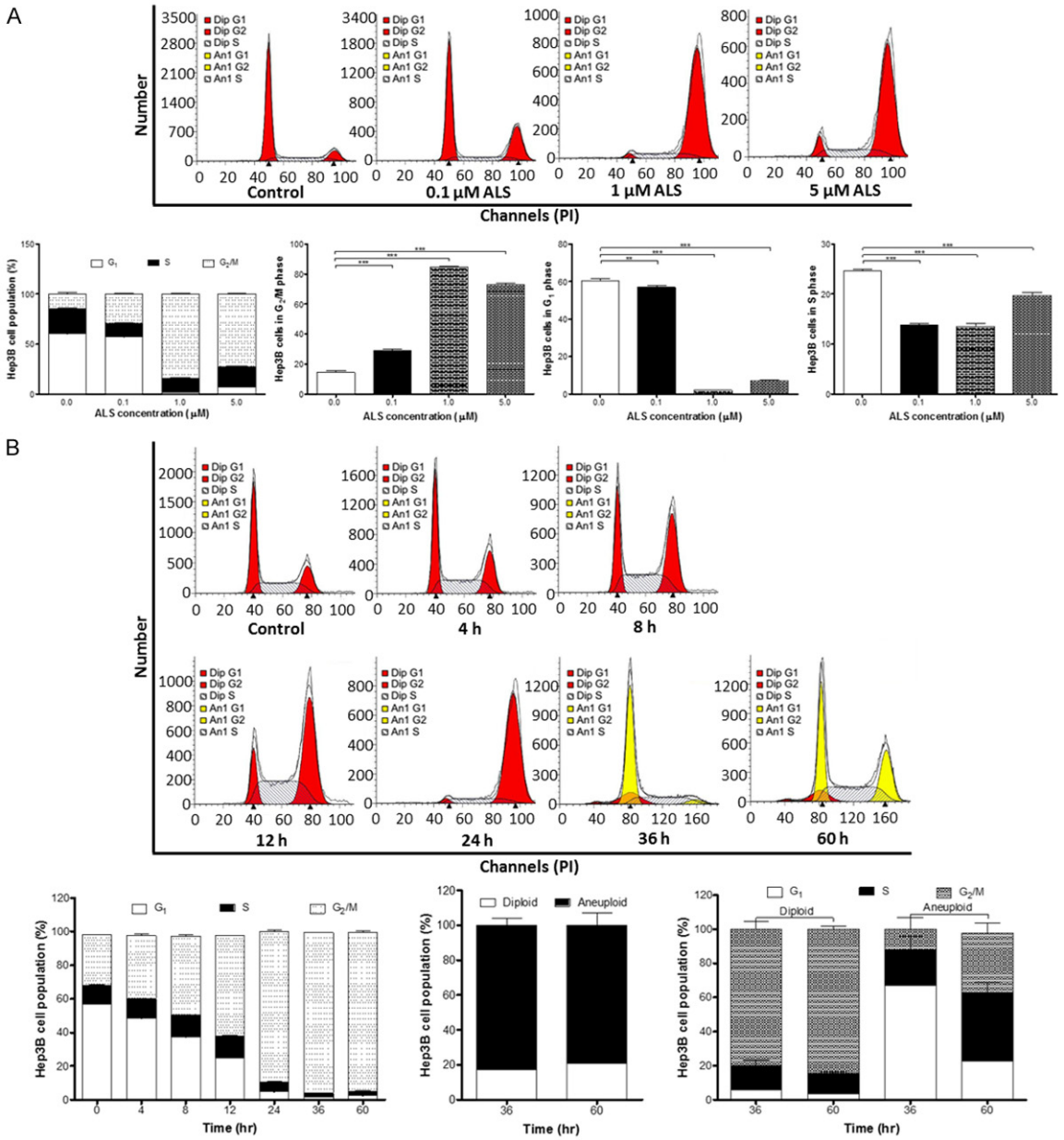

Figure 2. Effect of ALS on cell cycle distribution of Hep3B cells. Hep3B cells were treated with ALS at 0.1, 1, and 5 μM for 24 h (A), or treated with ALS at 1 μM for 4, 8, 12, 24, 36, and 60 h (B), and then subject to flow cytometric analysis. Representative flow cytometric plots of cell cycle distribution. Bar graphs show the percentage of Hep3B cells in G_1, S, and G_2/M phases. Data are the mean ± SD of three independent experiments. $*P < 0.05$, $**P < 0.001$, and $***P < 0.001$ by one-way ANOVA.

mulation of aneuploid in a concentration- and time-dependent manner.

ALS alters the expression of key cell cycle regulators in Hep3B cells

We next examine the effect of ALS on the expression levels of key regulators responsible for G_2 checkpoint in Hep3B cells using Western blotting assay. Although the total level of CDC2 and cyclin B1 increased significantly, there were also a remarkable alteration in the phosphorylation level of CDC2 and cyclin B1 when Hep3B cells were treated with ALS at 1 and 5 μM. Treatment of Hep3B cells with ALS at 1 and 5 μM led to an increase in the level of p-CDC2 (Tyr15) by 85.7% and 59.1% ($P < 0.001$, **Figure 3**), respectively, while led to a decrease in the

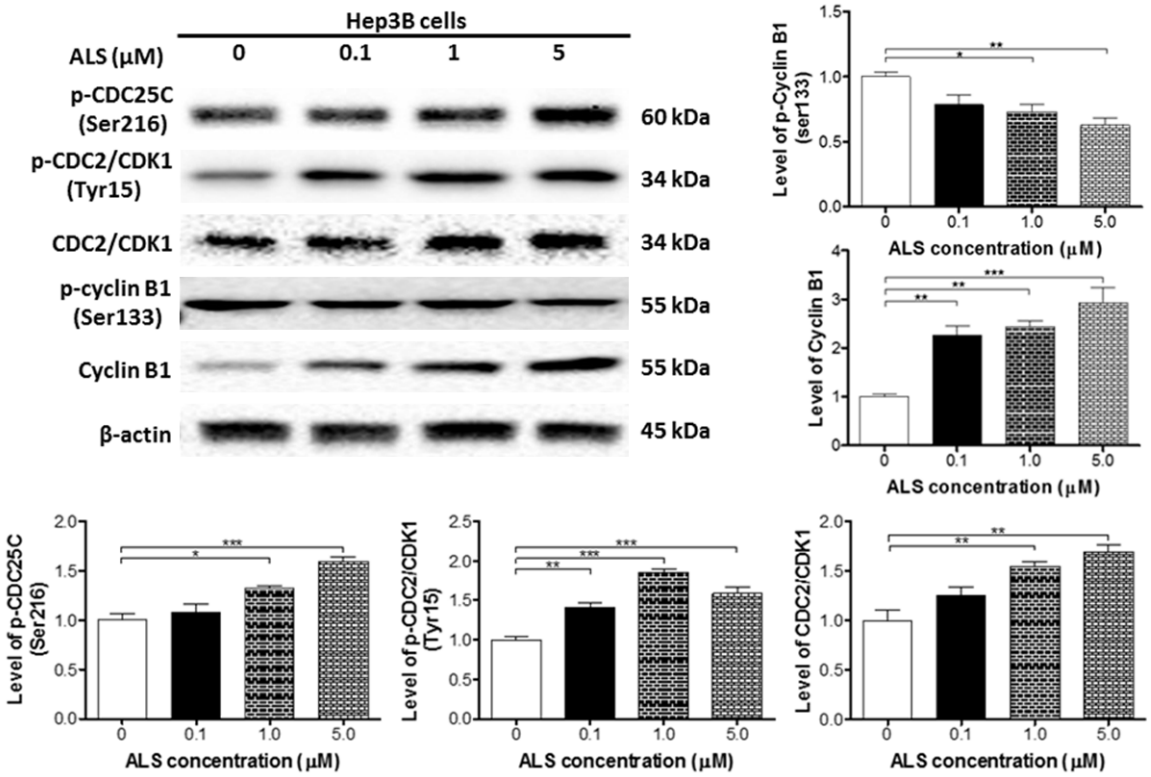

Figure 3. ALS modulates the expression of key proteins responsible for the G_2 checkpoint. Hep3B cells were incubated with ALS at 0.1, 1, and 5 μM for 24 h, and the protein samples were subject to Western blotting assay. Representative blots of p-CDC25C (Ser216), p-CDC2/CDK1 (Tyr15), CDC2/CDK1, p-cyclin B1 (Ser133), and cyclin B1. Bar graphs shows the relative level of the above proteins. β-Actin was used as the internal control. Data are the mean ± SD of three independent experiments. **P* < 0.05, ***P* < 0.001, and ****P* < 0.001 by one-way ANOVA.

level of p-cyclin B1 (ser133) by 27.1% and 37.3% (*P* < 0.05 or 0.01, **Figure 3**). Both the activation of p-CDC2 at Tyr15 and inhibition of p-cyclin B1 at ser133 resulted in inactivation of CDC2-cyclin B1 complex in Hep3B cells with p53 deletion. Besides, there was a 78.8% and 69.9% increase in the level of p-CDC25C at Ser216, a kinase responsible for the dephosphorylation of CDC2 at Tyr15, when Hep3B cells were treated with 1 and 5 μM ALS for 24 h (*P* < 0.05 or 0.001, **Figure 3**). These data demonstrate that ALS leads to G_2/M arrest and accumulation of aneuploid Hep3B cells via altering the expression of key cell cycle regulators.

ALS induces remarkable autophagy in Hep3B cells

To further test the anticancer activity of ALS, we examined the effect of ALS on programmed cell death in Hep3B cells. Although the IPA analysis revealed that both apoptosis signaling and myc-mediated apoptosis signaling pathway were regulated by ALS (Table S2), our flow cytometric data showed that the effect of ALS on apoptosis is weak (**Figure 4**). The IPA analysis results demonstrated the effect of ALS on nutrition and energy metabolic process, indicating the regulatory role of ALS in autophagy. Then flow cytometric analysis, LC3 conversion, beclin 1 and SQSTM1/p62 expression assay and puncta formation assay examined by confocal fluorescence microscopy were performed to test the effect of ALS on autophagy. As shown in **Figure 5A**, treatment on Hep3B cells with ALS significantly increased the percentage of autophagic cells dose- and time-dependently. Compared to the control cells (with basal level 9.8%), there was a 31.9% and 20.9% increase in autophagy when treated with ALS at 1 and 5 μM for 24 h, respectively (*P* < 0.001, **Figure 5A**). After incubation of Hep3B cell with ALS at 1 μM for 24, 36 and 60 h, the autophagy rate increased by 2.5-, 3.4- and 5.8-fold, respectively (*P* < 0.001, **Figure 5A**).

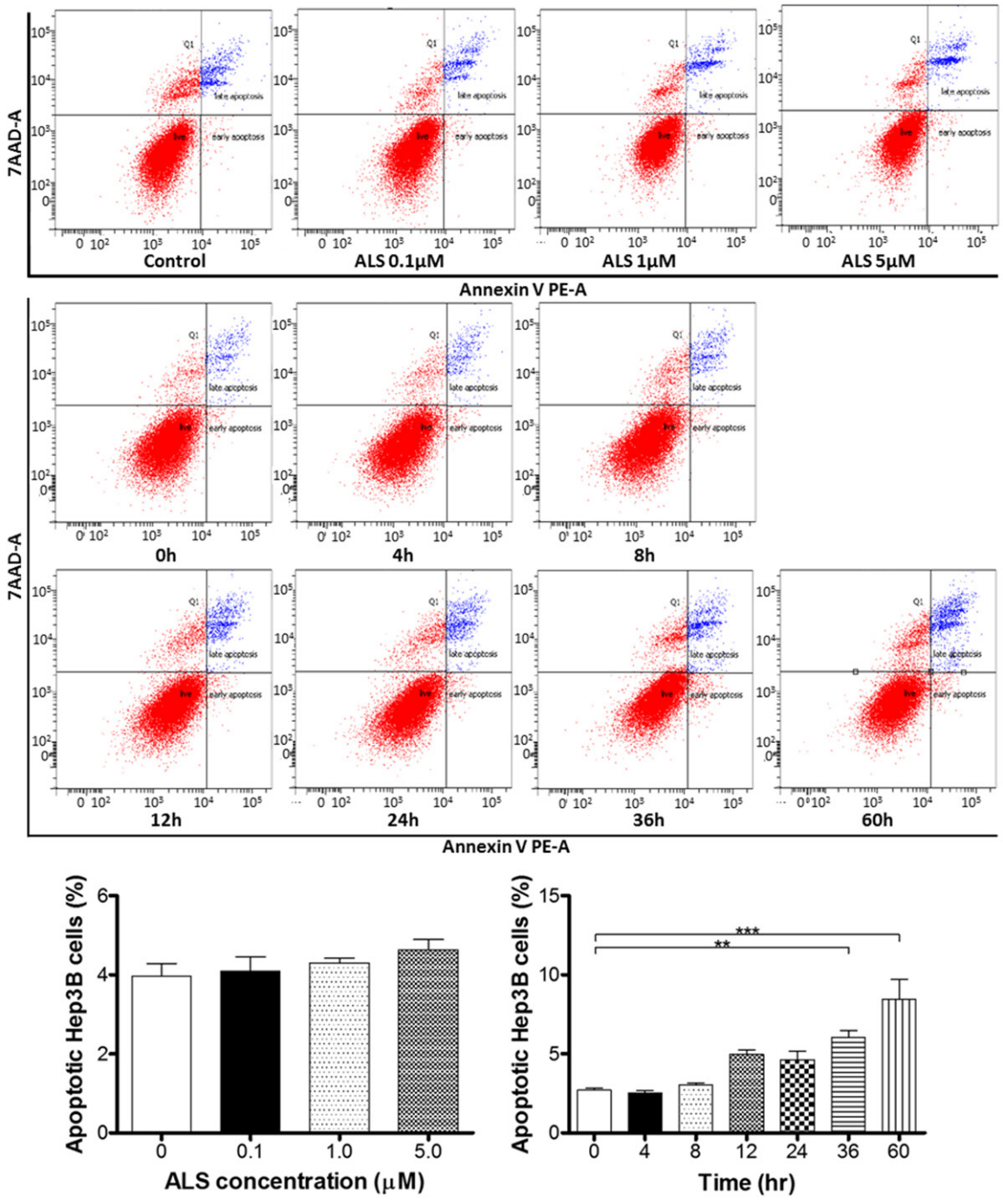

Figure 4. ALS exerts weak proapoptotic effect on Hep3B cells. Hep3B cells were incubated with ALS at 0.1, 1, and 5 μM for 24 h, or treated with ALS at 1 μM for 4, 8, 12, 24, 36, and 60 h, and then subject to flow cytometric analysis. Flow cytometric plots and percentage of specific cell populations (live, early apoptosis, and late apoptosis) in Hep3B cells. Bar graphs show the percentage of apoptotic Hep3B cells. Data are the mean ± SD of three independent experiments. ***$P < 0.001$ by one-way ANOVA.

As shown in **Figure 5B**, ALS treatment at 5 μM for 24 h increased the expression of LC3-II and beclin 1 by 85.9% and 22.0%, respectively ($P < 0.05$ or 0.01, **Figure 5B**), but decreased the expression of LC3-I and SQSTM1/p62 by 56.2% and 24.1%, respectively ($P < 0.05$, **Figure 5B**). The ratio of LC3-II/LC3-I was elevated 2.8-fold and 4.3-fold when Hep3B cells were treated

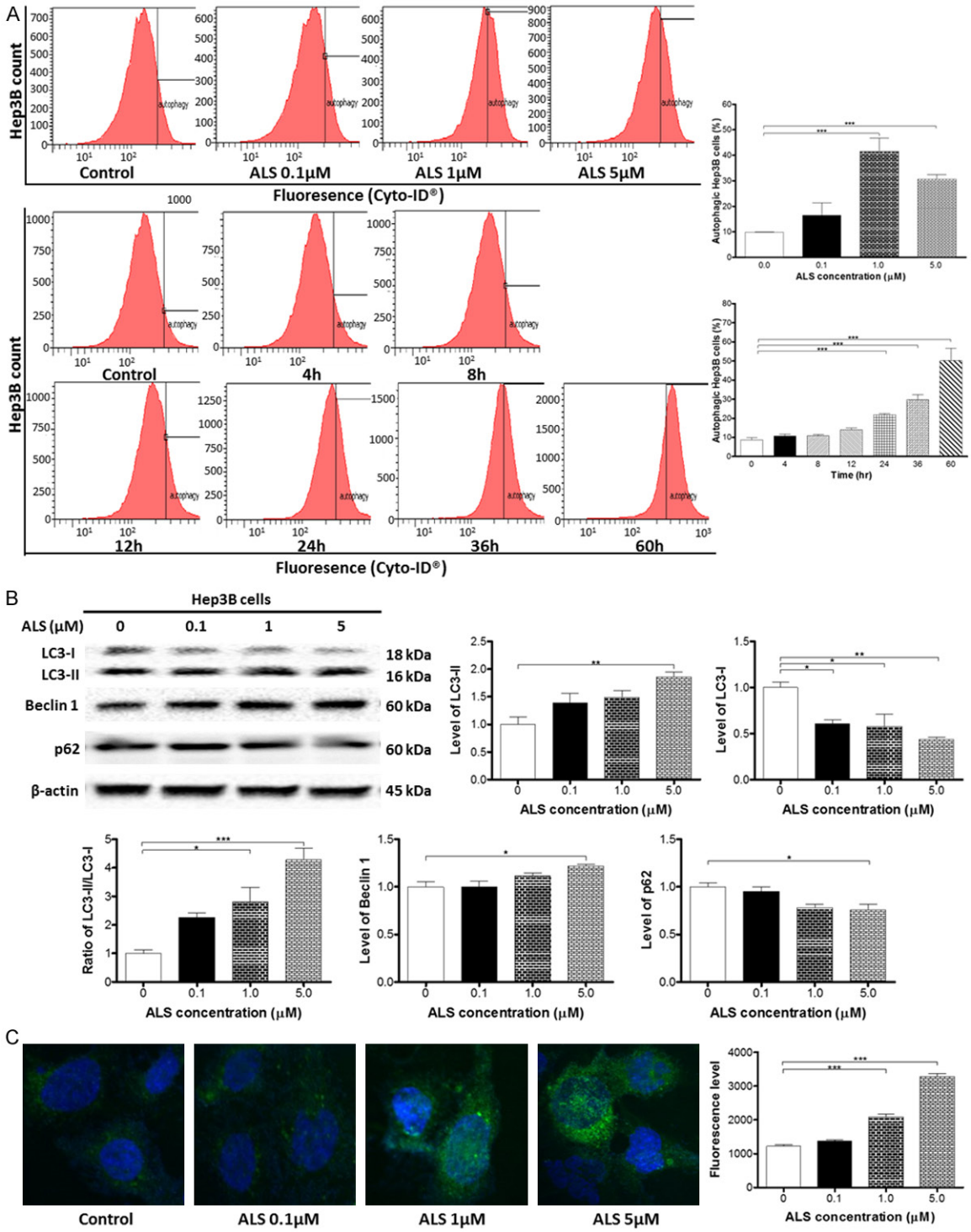

Figure 5. ALS induces autophagy in Hep3B cells. Hep3B cells were incubated with ALS at 0.1, 1, and 5 μM for 24 h, or treated with ALS at 1 μM for 4, 8, 12, 24, 36, and 60 h. Then cells were subject to confocal microscopic examination or flow cytometry analysis. The protein samples were subject to Western blot assay. A. Histograms show autophagy of Hep3B cells. Bar graphs showing the percentage of autophagic Hep3B cells. B. Representative blots of LC3-I, LC3-II, beclin 1, and p62 determined by western blotting. β-Actin was used as the internal control. Bar graphs show the relative level of the above proteins. C. Representative confocal microscopic images show autophagy of Hep3B cells. Bar graph showing the fluorescence level. Data are the mean ± SD of three independent experiments. $*P < 0.01$, $**P < 0.001$, and $***P < 0.001$ by one-way ANOVA.

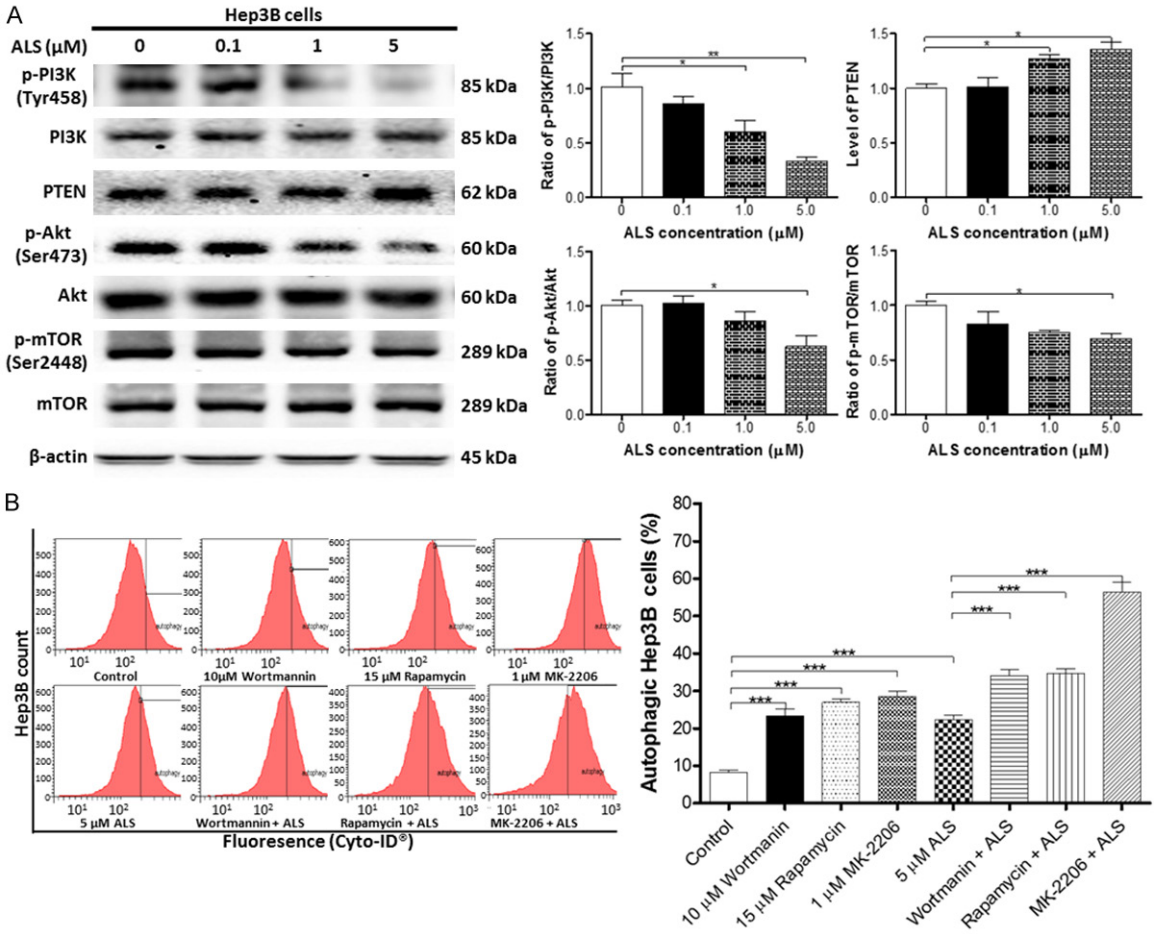

Figure 6. ALS induces autophagy with involvement of PI3K/Akt/mTOR signaling pathway. Hep3B cells were incubated with ALS at 0.1, 1, and 5 μM for 24 h, and the protein samples were subject to Western blot assay. A. Representative blots of phosphorylation level of PI3K, Akt, and mTOR and the total levels of PI3K, Akt, mTOR and PTEN determined by Western blotting assay. Bar graphs show the ratio of p-PI3K/PI3K, p-Akt/Akt, and p-mTOR/mTOR and the expression level of PTEN in Hep3B cells. β-Actin was used as the internal control. B. Hep3B cells were pretreated 1 h with WM (10 μM), MK-2206 (1 μM) or rapamycin (15 μM), co-treated with 5 μM ALS for a further 24 h and then subject to flow cytometric analysis. Histograms show autophagy of Hep3B cells. Bar graph showing the percentage of autophagic Hep3B cells. Data are the mean ± SD of three independent experiments. *$P < 0.05$, **$P < 0.001$, and ***$P < 0.001$ by one-way ANOVA.

with ALS at 1 and 5 μM for 24 h, respectively. The confocal microscopic examination showed that autophagic level was increased 1.7- and 2.7-fold when Hep3B cells were treated with ALS at 1 and 5 μM for 24 h, respectively ($P < 0.001$, **Figure 5C**). Taken together, these results demonstrate that ALS is a potent autophagy inducer in Hep3B cells.

ALS modulates the PI3K/Akt/mTOR pathway in Hep3B cells

Since the IPA analysis demonstrated the mTOR signaling, along with upstream PI3K/Akt signaling were regulated by ALS (Table S2, **Table 1** and Figure S4), we speculated that ALS induced autophagy with involvement of the well-known PI3K/Akt/mTOR pathway. We first examined the effect of ALS on the expression of this axis-related proteins and their phosphorylation levels. As shown in **Figure 6A**, ALS markedly inhibited the phosphorylation of PI3K at Tyr199, Akt at Ser473 and mTOR at Ser2448, but did not impact the expression of total PI3K, Akt and mTOR. ALS treatment at 5 μM for 24 h decreased the ratio of p-PI3K/PI3K, p-Akt/Akt, and p-mTOR/mTOR by 66.9%, 37.2% and 30.4%, respectively ($P < 0.05$ or 0.01, **Figure 6A**). In addition, treatment of Hep3B cells with 5 μM ALS for 24 h upregulated the expression

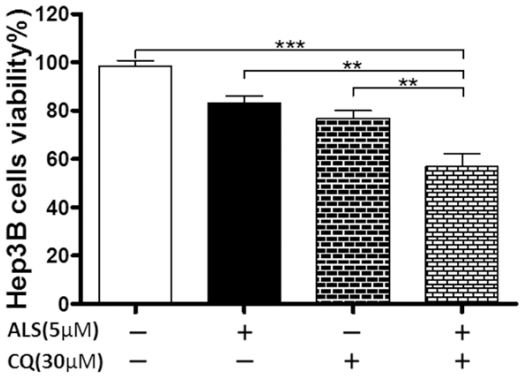

Figure 7. Inhibition of autophagy enhanced the anticancer activity of ALS in Hep3B cells. Hep3B were treated with 5 μM ALS or 30 μM chloroquine (CQ) alone, or coincubated with 5 μM ALS and 30 μM CQ for 24 h, then subject to the MTT assay. Bar graph showing the viability of Hep3B cells. Data are the mean ± SD of three independent experiments. $^{**}P < 0.001$ and $^{***}P < 0.001$ by one-way ANOVA.

of PTEN, the negative regulator of PI3K, by 35.5% ($P < 0.05$, **Figure 6A**).

We next used specific chemical inhibitors to validate the involvement of PI3K/Akt/mTOR pathway in ALS-induced autophagy. As shown in **Figure 6B**, co-incubation of ALS with WM (10 μM, a PI3K inhibitor), MK-2206 (1 μM, an Akt inhibitor) and rapamycin (15 μM, an mTOR inhibitor) enhanced ALS-induced autophagy, with autophagy level being elevated from 22.3% (5 μM ALS alone) to 34.2%, 56.5% and 34.7%, respectively ($P < 0.001$, **Figure 6B**). Collectively, these findings suggest that ALS induce autophagy via the PI3K/Akt/mTOR pathway in Hep3B cells.

Inhibition of autophagy enhances the anticancer activity of ALS in Hep3B cells

Finally, we explored the effect of inhibition of ALS-induced autophagy on the viability of Hep3B cells. As shown in **Figure 7**, inhibition of ALS-induced autophagy with CQ enhanced the cell-killing activity of ALS, with the viability of Hep3B cells decreased from 83.1% (5 μM ALS alone) or 76.9% (30 μM CQ alone) to 56.7% (5 μM ALS plus 30 μM CQ) ($P < 0.01$, **Figure 7**). These data suggest that autophagy inhibitor may augment the anticancer activity of ALS in Hep3B cells.

Discussion

Currently, HCC treatment guidelines recommend a multidisciplinary team for the clinical management and therapeutic options should be stage-dependent [39, 40]. HCC patients diagnosed in later stages are proposed to receive systemic therapy. To date, sorafenib remains the only drug approved for the therapy of inoperable or metastatic HCC. Although the SHARP and Oriental study have shown that sorafenib can delay tumor progression and prolong survival of patients with advanced HCC [12, 13], the efficacy of sorafenib is far from being satisfied. Acquired resistance of HCC to sorafenib is often observed. A series of clinical studies on new targeted agents (such as brivanib, sunitinib, linifanib, ramucirumab, everolimus and erlotinib) for HCC treatment have been conducted, but all these studies failed [9]. Investigation of other effective agents is urgently mandatory. A number of Aurora kinase inhibitors (AKIs) have been developed and tested in Phase I and II trials [41]. In the present study, we investigated the anticancer activity of ALS in Hep3B cells using a SILAC proteomic analysis. Our results demonstrated that ALS regulated a number of proteins and molecular signaling pathways, which involved various molecular and cellular functions with cellular growth and proliferation and cell death and survival among the top five. Subsequent cell-based validation studies showed that ALS treatment inhibited the proliferation and led to G_2/M phase arrest and accumulation of aneuploid Hep3B cells. ALS induced significantly autophagy via PI3K/Akt/mTOR signaling pathway, but it was a weak inducer of apoptosis in Hep3B cells.

SILAC is valuable in revealing the general proteomic responses to drug treatment [42]. In particular, it can be used to systemically and quantitatively assess the target network of drugs, and identify new biomarkers for the diagnosis and treatment of cancers [42, 43]. We conducted a SILAC-based proteomic study to identify the potential molecular targets of ALS in Hep3B cells. It revealed that those proteins and molecular signaling pathways regulated by ALS were largely involved in cellular growth and proliferation, cell death and survival, protein synthesis, gene expression and RNA post-transcriptional modification. The proteomic results suggest that ALS may target these signaling molecules to elicit its anticancer effects in the treatment of Hep3B cells.

Proper mitotic progression largely depends on the normal kinase activity of AURKA, while inhi-

bition of AURKA lead to improper mitotic events, including G_2/M phase arrest [44]. Our results demonstrated that ALS treatment inhibited the phosphorylation of AURKA at Thr288 in a concentration-dependent manner, followed by G_2/M phase arrest. This is consistent with the proteomic findings with regard to the remarkable role of ALS in the regulation of G_2/M DNA damage checkpoint. The effect of ALS on the cell cycle distribution in Hep3B cells was further confirmed with suppressed activity of CDC2-cyclin B1 complex. We observed that ALS treatment led to increased phosphorylation of CDC2 at Tyr15 and inhibition of cyclin B1 phosphorylation at Ser133 in Hep3B cells. The altered phosphorylation of CDC2 and cyclin B could result in inactivation of CDC2-cyclin B1 complex, finally leading to G_2/M arrest. We further detected the increased phosphorylation level of CDC25C at Ser216 by ALS, a kinase responsible for the dephosphorylation of CDC2 at Tyr15. Collectively, these data indicate that ALS induces G_2/M arrest in Hep3B cells via regulating key regulators of cell cycle.

Autophagy plays a critical role in providing energy for cellular renovation and maintaining intracellular hemostasis. Under most circumstances, autophagy represents a pro-survival process against apoptosis [45-48]. The PI3K/Akt/mTOR axis is a central pathway involved in autophagy through the regulation of cell growth, motility, protein synthesis, cell metabolism, cell survival, and cell death in response to various stimuli [49, 50]. PTEN inhibits Akt/mTOR and MAPK signaling, leading to cell death and growth regulation [51]. In the present study, our finding demonstrated that ALS treatment induced remarkable autophagy. The p-PI3K/PI3K, p-Akt/Akt ratio and p-mTOR/ mTOR were significantly decreased by ALS in a concentration-dependent manner in Hep3B cells. We also found that ALS induced remarkable increased the expression of PTEN. These findings indicate that ALS has a significant autophagy-inducing effect on Hep3B cells via inhibition of the PI3K/Akt/mTOR axis.

In the present study, ALS only exerted weak pro-apoptotic effect in Hep3B cells. The reasons for the weak inducing effect of ALS on apoptosis in Hep3B cells are unknown. Autophagy may suppress the apoptosis due to crosstalk and Hep3B cells may be resistant to initiation of apoptosis by ALS due to disabling of pro-apoptotic signals and activation of anti-apoptotic signals. The genetic heterogeneity of HCC may also contributes to this. Mutations of p53 as well as a deregulation between the expression of pro- and anti-apoptotic proteins of the Bcl-2 family are frequently observed in HCC. Our study showed that inhibition of ALS-induced autophagy enhanced its cell-killing activity, probably through augmented apoptosis and/or necrosis.

Recently, a study has shown that ALS is a substrate of P-glycoprotein, and inhibition of P-glycoprotein by verapamil increased ALS uptake in Caco2 and MKN45 cells [52]. These findings imply that combinational use with autophagy blockers or P-glycoprotein inhibitors may enhance the anticancer activity of ALS in Hep3B cells, a cell line with P-glycoprotein overexpression [53, 54]. Besides, transarterial infusion or chemoembolization with ALS might be an alternative to systemic administration, since local concentration of drug could be increased dramatically using the above two methods [55]. Combined use of ALS with cytotoxic agents may be an alternative strategy to enhance its efficacy.

Conclusions

This study shows that ALS regulates a number of functional proteins and molecular signaling pathways, ALS inhibits cell proliferation, induces cell-cycle arrest and autophagy. More studies are warranted to investigate the role of ALS in the treatment of HCC. Proper combinational therapy may enhance the efficacy of ALS for HCC.

Disclosure of conflict of interest

None.

Authors' contribution

Participated in research design: Qiaohua Zhu, Zhi-Wei Zhou, Meihua Luo, Chengyu Zhou, Zhi-Xu He, Xinfa Yu, & Shu-Feng Zhou; Conducted experiments: Qiaohua Zhu, Zhi-Wei Zhou, Meihua Luo, & Chengyu Zhou; Performed data analysis: Qiaohua Zhu, Zhi-Wei Zhou, Meihua Luo, & Chengyu Zhou; Wrote or contributed to the writing of the manuscript: Qiaohua Zhu, Zhi-Wei Zhou, Meihua Luo, Chengyu Zhou, Zhi-Xu He, Xinfa Yu, & Shu-Feng Zhou.

Address correspondence to: Dr. Shufeng Zhou, Department of Bioengineering and Biotechnology, College of Chemical Engineering, Huaqiao University, 668 Jimei Blvd., Xiamen 361021, Fujian, China. E-mail: szhou@hqu.edu.cn; Dr. Xinfa Yu, Department of Oncology and Interventional Radiology, Shunde Hospital, Southern Medical University, Shunde 528300, Guangdong, China. E-mail: irist_dryu@163.com

References

[1] Torre LA, Bray F, Siegel RL, Ferlay J, Lortet-Tieulent J and Jemal A. Global cancer statistics, 2012. CA Cancer J Clin 2015; 65: 87-108.

[2] El-Serag HB. Hepatocellular carcinoma. N Engl J Med 2011; 365: 1118-1127.

[3] Chacko S and Samanta S. "Hepatocellular carcinoma: A life-threatening disease". Biomed Pharmacother 2016; 84: 1679-1688.

[4] Mazzanti R, Arena U and Tassi R. Hepatocellular carcinoma: where are we? World J Exp Med 2016; 6: 21-36.

[5] Llovet JM, Zucman-Rossi J, Pikarsky E, Sangro B, Schwartz M, Sherman M and Gores G. Hepatocellular carcinoma. Nat Rev Dis Primers 2016; 2: 16018.

[6] Grandhi MS, Kim AK, Ronnekleiv-Kelly SM, Kamel IR, Ghasebeh MA and Pawlik TM. Hepatocellular carcinoma: from diagnosis to treatment. Surg Oncol 2016; 25: 74-85.

[7] Mazzoccoli G, Miele L, Oben J, Grieco A and Vinciguerra M. Biology, epidemiology, clinical aspects of hepatocellular carcinoma and the role of sorafenib. Curr Drug Targets 2016; 17: 783-799.

[8] Diaz-Gonzalez A, Reig M and Bruix J. Treatment of hepatocellular carcinoma. Dig Dis 2016; 34: 597-602.

[9] Gong XL and Qin SK. Progress in systemic therapy of advanced hepatocellular carcinoma. World J Gastroenterol 2016; 22: 6582-6594.

[10] Qin S, Bai Y, Lim HY, Thongprasert S, Chao Y, Fan J, Yang TS, Bhudhisawasdi V, Kang WK, Zhou Y, Lee JH and Sun Y. Randomized, multicenter, open-label study of oxaliplatin plus fluorouracil/leucovorin versus doxorubicin as palliative chemotherapy in patients with advanced hepatocellular carcinoma from Asia. J Clin Oncol 2013; 31: 3501-3508.

[11] Qin S, Cheng Y, Liang J, Shen L, Bai Y, Li J, Fan J, Liang L, Zhang Y, Wu G, Rau KM, Yang TS, Jian Z, Liang H and Sun Y. Efficacy and safety of the FOLFOX4 regimen versus doxorubicin in Chinese patients with advanced hepatocellular carcinoma: a subgroup analysis of the EACH study. Oncologist 2014; 19: 1169-1178.

[12] Llovet JM, Ricci S, Mazzaferro V, Hilgard P, Gane E, Blanc JF, de Oliveira AC, Santoro A, Raoul JL, Forner A, Schwartz M, Porta C, Zeuzem S, Bolondi L, Greten TF, Galle PR, Seitz JF, Borbath I, Haussinger D, Giannaris T, Shan M, Moscovici M, Voliotis D, Bruix J; SHARP Investigators Study Group. Sorafenib in advanced hepatocellular carcinoma. N Engl J Med 2008; 359: 378-390.

[13] Cheng AL, Kang YK, Chen Z, Tsao CJ, Qin S, Kim JS, Luo R, Feng J, Ye S, Yang TS, Xu J, Sun Y, Liang H, Liu J, Wang J, Tak WY, Pan H, Burock K, Zou J, Voliotis D and Guan Z. Efficacy and safety of sorafenib in patients in the Asia-Pacific region with advanced hepatocellular carcinoma: a phase III randomised, double-blind, placebo-controlled trial. Lancet Oncol 2009; 10: 25-34.

[14] von Felden J, Schulze K, Gil-Ibanez I, Werner T and Wege H. First- and second-line targeted systemic therapy in hepatocellular carcinoma-an update on patient selection and response evaluation. Diagnostics (Basel) 2016; 6.

[15] Brito AF, Abrantes AM, Tralhao JG and Botelho MF. Targeting hepatocellular carcinoma: what did we discover so far? Oncol Rev 2016; 10: 302.

[16] Fu J, Bian M, Jiang Q and Zhang C. Roles of Aurora kinases in mitosis and tumorigenesis. Mol Cancer Res 2007; 5: 1-10.

[17] Li JJ and Li SA. Mitotic kinases: the key to duplication, segregation, and cytokinesis errors, chromosomal instability, and oncogenesis. Pharmacol Ther 2006; 111: 974-984.

[18] Quartuccio SM and Schindler K. Functions of Aurora kinase C in meiosis and cancer. Front Cell Dev Biol 2015; 3: 50.

[19] Jeng YM, Peng SY, Lin CY and Hsu HC. Overexpression and amplification of Aurora-A in hepatocellular carcinoma. Clin Cancer Res 2004; 10: 2065-2071.

[20] Lin ZZ, Jeng YM, Hu FC, Pan HW, Tsao HW, Lai PL, Lee PH, Cheng AL and Hsu HC. Significance of Aurora B overexpression in hepatocellular carcinoma. Aurora B Overexpression in HCC. BMC Cancer 2010; 10: 461.

[21] Zhang K, Chen J, Chen D, Huang J, Feng B, Han S, Chen Y, Song H, De W, Zhu Z, Wang R and Chen L. Aurora-A promotes chemoresistance in hepatocelluar carcinoma by targeting NF-kappaB/microRNA-21/PTEN signaling pathway. Oncotarget 2014; 5: 12916-12935.

[22] Durlacher CT, Li ZL, Chen XW, He ZX and Zhou SF. An update on the pharmacokinetics and pharmacodynamics of alisertib, a selective Aurora kinase A inhibitor. Clin Exp Pharmacol Physiol 2016; 43: 585-601.

[23] Gorgun G, Calabrese E, Hideshima T, Ecsedy J, Perrone G, Mani M, Ikeda H, Bianchi G, Hu Y, Cirstea D, Santo L, Tai YT, Nahar S, Zheng M, Bandi M, Carrasco RD, Raje N, Munshi N, Rich-

ardson P and Anderson KC. A novel Aurora-A kinase inhibitor MLN8237 induces cytotoxicity and cell-cycle arrest in multiple myeloma. Blood 2010; 115: 5202-5213.

[24] Maris JM, Morton CL, Gorlick R, Kolb EA, Lock R, Carol H, Keir ST, Reynolds CP, Kang MH, Wu J, Smith MA and Houghton PJ. Initial testing of the aurora kinase A inhibitor MLN8237 by the Pediatric Preclinical Testing Program (PPTP). Pediatr Blood Cancer 2010; 55: 26-34.

[25] Tomita M and Mori N. Aurora A selective inhibitor MLN8237 suppresses the growth and survival of HTLV-1-infected T-cells in vitro. Cancer Sci 2010; 101: 1204-1211.

[26] Ding YH, Zhou ZW, Ha CF, Zhang XY, Pan ST, He ZX, Edelman JL, Wang D, Yang YX, Zhang X, Duan W, Yang T, Qiu JX and Zhou SF. Alisertib, an Aurora kinase A inhibitor, induces apoptosis and autophagy but inhibits epithelial to mesenchymal transition in human epithelial ovarian cancer cells. Drug Des Devel Ther 2015; 9: 425-464.

[27] Wang F, Li H, Yan XG, Zhou ZW, Yi ZG, He ZX, Pan ST, Yang YX, Wang ZZ, Zhang X, Yang T, Qiu JX and Zhou SF. Alisertib induces cell cycle arrest and autophagy and suppresses epithelial-to-mesenchymal transition involving PI3K/Akt/mTOR and sirtuin 1-mediated signaling pathways in human pancreatic cancer cells. Drug Des Devel Ther 2015; 9: 575-601.

[28] Li JP, Yang YX, Liu QL, Pan ST, He ZX, Zhang X, Yang T, Chen XW, Wang D, Qiu JX and Zhou SF. The investigational Aurora kinase A inhibitor alisertib (MLN8237) induces cell cycle G2/M arrest, apoptosis, and autophagy via p38 MAPK and Akt/mTOR signaling pathways in human breast cancer cells. Drug Des Devel Ther 2015; 9: 1627-1652.

[29] Niu NK, Wang ZL, Pan ST, Ding HQ, Au GH, He ZX, Zhou ZW, Xiao G, Yang YX, Zhang X, Yang T, Chen XW, Qiu JX and Zhou SF. Pro-apoptotic and pro-autophagic effects of the Aurora kinase A inhibitor alisertib (MLN8237) on human osteosarcoma U-2 OS and MG-63 cells through the activation of mitochondria-mediated pathway and inhibition of p38 MAPK/PI3K/Akt/mTOR signaling pathway. Drug Des Devel Ther 2015; 9: 1555-1584.

[30] Ren BJ, Zhou ZW, Zhu DJ, Ju YL, Wu JH, Ouyang MZ, Chen XW and Zhou SF. Alisertib induces cell cycle arrest, apoptosis, autophagy and suppresses EMT in HT29 and Caco-2 cells. Int J Mol Sci 2015; 17: 41.

[31] Shu LP, Zhou ZW, Zi D, He ZX and Zhou SF. A SILAC-based proteomics elicits the molecular interactome of alisertib (MLN8237) in human erythroleukemia K562 cells. Am J Transl Res 2015; 7: 2442-2461.

[32] Yuan CX, Zhou ZW, Yang YX, He ZX, Zhang X, Wang D, Yang T, Wang NJ, Zhao RJ and Zhou SF. Inhibition of mitotic Aurora kinase A by alisertib induces apoptosis and autophagy of human gastric cancer AGS and NCI-N78 cells. Drug Des Devel Ther 2015; 9: 487-508.

[33] Qiu JX, Zhou ZW, He ZX, Zhao RJ, Zhang X, Yang L, Zhou SF and Mao ZF. Plumbagin elicits differential proteomic responses mainly involving cell cycle, apoptosis, autophagy, and epithelial-to-mesenchymal transition pathways in human prostate cancer PC-3 and DU145 cells. Drug Des Devel Ther 2015; 9: 349-417.

[34] Li J, Liu R, Lei Y, Wang K, Lau QC, Xie N, Zhou S, Nie C, Chen L, Wei Y and Huang C. Proteomic analysis revealed association of aberrant ROS signaling with suberoylanilide hydroxamic acid-induced autophagy in Jurkat T-leukemia cells. Autophagy 2010; 6: 711-724.

[35] Li ZL and Zhou SF. A SILAC-based approach elicits the proteomic responses to vancomycin-associated nephrotoxicity in human proximal tubule epithelial HK-2 Cells. Molecules 2016; 21: 148.

[36] Niu NK, Yin JJ, Yang YX, Wang ZL, Zhou ZW, He ZX, Chen XW, Zhang X, Duan W, Yang T and Zhou SF. Novel targeting of PEGylated liposomes for codelivery of TGF-β1 siRNA and four antitubercular drugs to human macrophages for the treatment of mycobacterial infection: a quantitative proteomic study. Drug Des Devel Ther 2015; 9: 4441-4470.

[37] Pan ST, Qin Y, Zhou ZW, He ZX, Zhang X, Yang T, Yang YX, Wang D, Zhou SF and Qiu JX. Plumbagin suppresses epithelial to mesenchymal transition and stemness via inhibiting Nrf2-mediated signaling pathway in human tongue squamous cell carcinoma cells. Drug Des Devel Ther 2015; 9: 5511-5551.

[38] Pan ST, Zhou ZW, He ZX, Zhang X, Yang T, Yang YX, Wang D, Qiu JX and Zhou SF. Proteomic response to 5,6-dimethylxanthenone 4-acetic acid (DMXAA, vadimezan) in human non-small cell lung cancer A549 cells determined by the stable-isotope labeling by amino acids in cell culture (SILAC) approach. Drug Des Devel Ther 2015; 9: 937-968.

[39] Guy J, Kelley RK, Roberts J, Kerlan R, Yao F and Terrault N. Multidisciplinary management of hepatocellular carcinoma. Clin Gastroenterol Hepatol 2012; 10: 354-362.

[40] Kaseb AO, Abaza YM and Roses RE. Multidisciplinary management of hepatocellular carcinoma. Recent Results Cancer Res 2013; 190: 247-259.

[41] Cicenas J. The Aurora kinase inhibitors in cancer research and therapy. J Cancer Res Clin Oncol 2016; 142: 1995-2012.

[42] Ong SE and Mann M. Stable isotope labeling by amino acids in cell culture for quantitative proteomics. Methods Mol Biol 2007; 359: 37-52.
[43] Ong SE and Mann M. A practical recipe for stable isotope labeling by amino acids in cell culture (SILAC). Nat Protoc 2006; 1: 2650-2660.
[44] Dar AA, Goff LW, Majid S, Berlin J and El-Rifai W. Aurora kinase inhibitors - rising stars in cancer therapeutics? Mol Cancer Ther 2010; 9: 268-278.
[45] Zhao GX, Pan H, Ouyang DY and He XH. The critical molecular interconnections in regulating apoptosis and autophagy. Ann Med 2015; 47: 305-315.
[46] Rabinowitz JD and White E. Autophagy and metabolism. Science 2010; 330: 1344-1348.
[47] Yang Z and Klionsky DJ. Eaten alive: a history of macroautophagy. Nat Cell Biol 2010; 12: 814-822.
[48] Mizushima N and Komatsu M. Autophagy: renovation of cells and tissues. Cell 2011; 147: 728-741.
[49] Rodon J, Dienstmann R, Serra V and Tabernero J. Development of PI3K inhibitors: lessons learned from early clinical trials. Nat Rev Clin Oncol 2013; 10: 143-153.
[50] Taylor RC, Cullen SP and Martin SJ. Apoptosis: controlled demolition at the cellular level. Nat Rev Mol Cell Biol 2008; 9: 231-241.
[51] Mester J and Eng C. When overgrowth bumps into cancer: the PTEN-opathies. Am J Med Genet C Semin Med Genet 2013; 163C: 114-121.
[52] Goos JA, Verbeek J, Geldof AA, Hiemstra AC, van de Wiel MA, Adamzek KA, Delis-Van Diemen PM, Stroud SG, Bradley DP, Meijer GA, Hoekstra OS, Fijneman RJ and Windhorst AD. Molecular imaging of aurora kinase A (AURKA) expression: synthesis and preclinical evaluation of radiolabeled alisertib (MLN8237). Nucl Med Biol 2016; 43: 63-72.
[53] Meena AS, Sharma A, Kumari R, Mohammad N, Singh SV and Bhat MK. Inherent and acquired resistance to paclitaxel in hepatocellular carcinoma: molecular events involved. PLoS One 2013; 8: e61524.
[54] Yang T, Zheng ZM, Li XN, Li ZF, Wang Y, Geng YF, Bai L and Zhang XB. MiR-223 modulates multidrug resistance via downregulation of ABCB1 in hepatocellular carcinoma cells. Exp Biol Med (Maywood) 2013; 238: 1024-1032.
[55] Saraswat VA, Pandey G and Shetty S. Treatment algorithms for managing hepatocellular carcinoma. J Clin Exp Hepatol 2014; 4: S80-89.

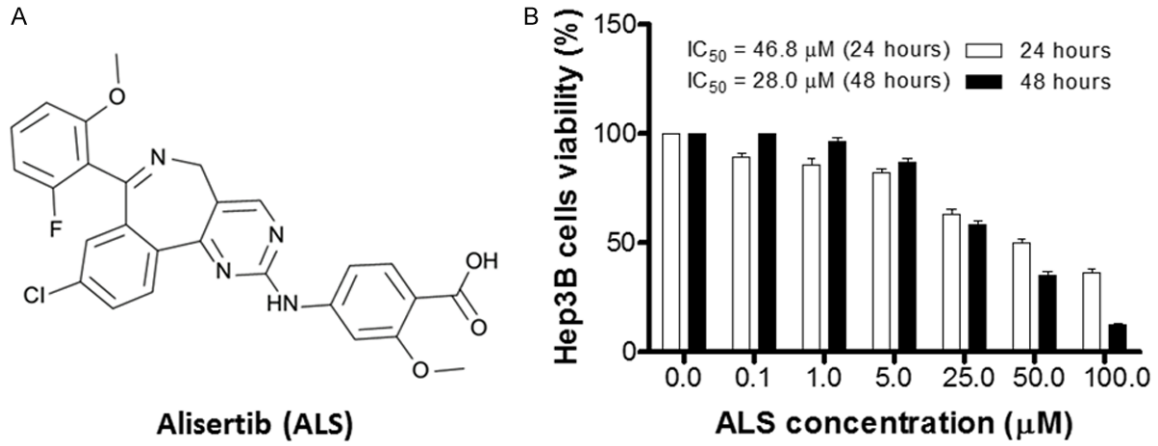

Figure S1. Chemical structure and cytotoxicity of ALS. A. The chemical structure of ALS. B. Cytotoxicity of ALS towards Hep3B cells determined by MTT assay.

Table S1. The 566 protein molecules regulated by alisertib in Hep3B cells

No.	Protein ID	Protein Name	Gene Name	H/L Ratio
1	Q9P258	Protein RCC2	*RCC2*	1.60
2	H7C457	Collagen α-1 (XVIII) chain	*COL18A1*	1.54
3	P52292	Importin subunit α-1	*KPNA2*	1.54
4	P35613	Basigin	*BSG*	1.46
5	Q15417	Calponin-3	*CNN3*	1.34
6	P09960	Leukotriene A_4 hydrolase	*LTA4H*	1.34
7	Q96FW1	Ubiquitin thioesterase OTUB1	*OTUB1*	1.33
8	O14818	Proteasome subunit α type-7	*PSMA7*	1.32
9	P38117	Electron transfer flavoprotein subunit β	*ETFB*	1.31
10	P35579	Myosin-9	*MYH9*	1.31
11	E7EV56	Pericentriolar material 1 protein	*PCM1*	1.30
12	P13284	γ-Interferon-inducible lysosomal thiol reductase	*IFI30*	1.30
13	P28482	Mitogen-activated protein kinase 1	*MAPK1*	1.30
14	Q01581	Hydroxymethylglutaryl-CoA synthase, cytoplasmic	*HMGCS1*	1.30
15	O43175	D-3-phosphoglycerate dehydrogenase	*PHGDH*	1.28
16	P23381	Tryptophan--tRNA ligase, cytoplasmic	*WARS*	1.27
17	C9JZR2	Catenin δ-1	*CTNND1*	1.27
18	P34897	Serine hydroxymethyltransferase, mitochondrial	*SHMT2*	1.27
19	P31153	S-adenosylmethionine synthase isoform type-2	*MAT2A*	1.27
20	P51149	Ras-related protein Rab-7a	*RAB7A*	1.25
21	O43809	Cleavage and polyadenylation specificity factor subunit 5	*NUDT21*	1.25
22	Q9Y617	Phosphoserine aminotransferase	*PSAT1*	1.24
23	F5GWX5	Chromodomain-helicase-DNA-binding protein 4	*CHD4*	1.24
24	Q6AWB1	Dynactin subunit 1	*DKFZp686E0752*	1.23
25	Q13492	Phosphatidylinositol-binding clathrin assembly protein	*PICALM*	1.23
26	P52907	F-actin-capping protein subunit α-1	*CAPZA1*	1.22
27	Q9UGI8	Testin	*TES*	1.22
28	P25325	3-Mercaptopyruvate sulfurtransferase	*MPST*	1.21
29	Q9UBT2	SUMO-activating enzyme subunit 2	*UBA2*	1.21
30	P11216	Glycogen phosphorylase, brain form	*PYGB*	1.21
31	Q03252	Lamin-B2	*LMNB2*	1.20
32	P31930	Cytochrome *b*-c1 complex subunit 1, mitochondrial	*UQCRC1*	1.20
33	H3BQZ7	Heterogeneous nuclear ribonucleoprotein U-like protein 2	*hCG_2044799*	1.20
34	P11766	Alcohol dehydrogenase class-3	*ADH5*	1.19
35	E9PB90	Hexokinase-2	*HK2*	1.19
36	P36507	Dual specificity mitogen-activated protein kinase kinase 2	*MAP2K2*	1.18
37	P41091	Eukaryotic translation initiation factor 2 subunit 3	*EIF2S3*	1.18
38	Q07065	Cytoskeleton-associated protein 4	*CKAP4*	1.18
39	P19105	Myosin regulatory light chain 12A	*MYL12A*	1.18
40	O95865	N(G),N(G)-dimethylarginine dimethylaminohydrolase 2	*DDAH2*	1.17
41	Q13200	26S proteasome non-ATPase regulatory subunit 2	*PSMD2*	1.17
42	Q9Y4L1	Hypoxia up-regulated protein 1	*HYOU1*	1.16
43	P50454	Serpin H1	*SERPINH1*	1.16
44	P08107	Heat shock 70 kDa protein 1A/1B	*HSPA1A*	1.15
45	Q99832	T-complex protein 1 subunit η	*CCT7*	1.15
46	O14980	Exportin-1	*XPO1*	1.14
47	Q9NYU2	UDP-glucose:glycoprotein glucosyltransferase 1	*UGGT1*	1.14
48	P48735	Isocitrate dehydrogenase [NADP], mitochondrial	*IDH2*	1.14
49	Q9UJZ1	Stomatin-like protein 2, mitochondrial	*STOML2*	1.14
50	P68402	Platelet-activating factor acetylhydrolase IB subunit β	*PAFAH1B2*	1.14
51	P04080	Cystatin-B	*CSTB*	1.13
52	P09417	Dihydropteridine reductase	*QDPR*	1.13
53	Q12905	Interleukin enhancer-binding factor 2	*ILF2*	1.13
54	Q9Y3I0	tRNA-splicing ligase RtcB homolog	*C22orf28*	1.13
55	O43390	Heterogeneous nuclear ribonucleoprotein R	*HNRNPR*	1.13

56	Q9Y5B9	FACT complex subunit SPT16	*SUPT16H*	1.13
57	F6SBX2	Isoleucine-tRNA ligase, mitochondrial	*IARS2*	1.12
58	P06493	Cyclin-dependent kinase 1	*CDK1*	1.12
59	P42167	Lamina-associated polypeptide 2, isoforms β/γ	*TMPO*	1.12
60	P30040	Endoplasmic reticulum resident protein 29	*ERP29*	1.12
61	E9PPJ5	Midkine	*MDK*	1.12
62	Q8NE71	ATP-binding cassette sub-family F member 1	*ABCF1*	1.12
63	P31948	Stress-induced-phosphoprotein 1	*STIP1*	1.12
64	H3BT13	Small nuclear ribonucleoprotein Sm D3	*SNRPD3*	1.12
65	Q96KP4	Cytosolic non-specific dipeptidase	*CNDP2*	1.12
66	P62158	Calmodulin	*CALM1*	1.12
67	P19338	Nucleolin	*NCL*	1.11
68	Q07955	Serine/arginine-rich splicing factor 1	*SRSF1*	1.11
69	H0Y3Y4	Septin-7	7-Sep	1.11
70	P30084	Enoyl-CoA hydratase, mitochondrial	*ECHS1*	1.11
71	O00303	Eukaryotic translation initiation factor 3 subunit F	*EIF3F*	1.11
72	O75874	Isocitrate dehydrogenase [NADP] cytoplasmic	*IDH1*	1.11
73	P11413	Glucose-6-phosphate 1-dehydrogenase	*G6PD*	1.11
74	P05455	Lupus La protein	*SSB*	1.11
75	Q9P2E9	Ribosome-binding protein 1	*RRBP1*	1.11
76	Q9UK76	Hematological and neurological expressed 1 protein	*HN1*	1.11
77	P35241	Radixin	*RDX*	1.11
78	Q96AE4	Far upstream element-binding protein 1	*FUBP1*	1.10
79	H0YLC2	Proteasome subunit α type	*PSMA4*	1.10
80	D6RA82	Annexin	*ANXA3*	1.10
81	Q15019	Septin-2	2-Sep	1.10
82	P11021	78 kDa glucose-regulated protein	*HSPA5*	1.10
83	P37837	Transaldolase	*TALDO1*	1.10
84	H0YD73	26S proteasome non-ATPase regulatory subunit 13	*PSMD13*	1.10
85	Q9H4A6	Golgi phosphoprotein 3	*GOLPH3*	1.10
86	P14625	Endoplasmin	*HSP90B1*	1.10
87	E9PGT1	Translin	*TSN*	1.10
88	Q9HC35	Echinoderm microtubule-associated protein-like 4	*EML4*	1.10
89	Q9H307	Pinin	*PNN*	1.09
90	O43776	Asparagine-tRNA ligase, cytoplasmic	*NARS*	1.09
91	P82979	SAP domain-containing ribonucleoprotein	*SARNP*	1.09
92	P22314	Ubiquitin-like modifier-activating enzyme 1	*UBA1*	1.08
93	Q96PK6	RNA-binding protein 14	*RBM14*	1.08
94	P22626	Heterogeneous nuclear ribonucleoproteins A2/B1	*HNRNPA2B1*	1.08
95	P08574	Cytochrome c1, heme protein, mitochondrial	*CYC1*	1.08
96	E9PCY7	Heterogeneous nuclear ribonucleoprotein H	*HNRNPH1*	1.08
97	P08238	Heat shock protein HSP 90-β	*HSP90AB1*	1.08
98	P34932	Heat shock 70 kDa protein 4	*HSPA4*	1.08
99	A6PVH9	Copine-1	*CPNE1*	1.08
100	P12270	Nucleoprotein TPR	*TPR*	1.08
101	P30044	Peroxiredoxin-5, mitochondrial	*PRDX5*	1.08
102	Q9UBM7	7-Dehydrocholesterol reductase	*DHCR7*	1.08
103	G8JLD5	Dynamin-1-like protein	*DNM1L*	1.08
104	B4DGU4	Catenin β-1	*CTNNB1*	1.08
105	P07814	Bifunctional glutamate/proline-tRNA ligase	*EPRS*	1.08
106	D6RFM5	Succinate dehydrogenase [ubiquinone] flavoprotein subunit, mitochondrial	*SDHA*	1.08
107	P48643	T-complex protein 1 subunit epsilon	*CCT5*	1.07
108	P55735	Protein SEC13 homolog	*SEC13*	1.07
109	H3BN98	40S ribosomal protein S15a	*ARL6IP1*	1.07
110	E7EMD0	NADPH-cytochrome P450 reductase	*POR*	1.07
111	F5H018	GTP-binding nuclear protein Ran	*RAN*	1.07
112	P04844	Dolichyl-diphosphooligosaccharide-protein glycosyltransferase subunit 2	*RPN2*	1.07

113	P11387	DNA topoisomerase 1	*TOP1*	1.07
114	P23246	Splicing factor, proline- and glutamine-rich	*SFPQ*	1.07
115	Q14974	Importin subunit β-1	*KPNB1*	1.07
116	P68371	Tubulin β-4B chain	*TUBB4B*	1.07
117	F8W6I7	Heterogeneous nuclear ribonucleoprotein A1	*HNRNPA1*	1.07
118	Q15691	Microtubule-associated protein RP/EB family member 1	*MAPRE1*	1.07
119	P11047	Laminin subunit γ-1	*LAMC1*	1.07
120	P31689	DnaJ homolog subfamily A member 1	*DNAJA1*	1.06
121	E9PEJ4	Dihydrolipoyllysine-residue acetyltransferase component of pyruvate dehydrogenase complex, mitochondrial	*DLAT*	1.06
122	O43823	A-kinase anchor protein 8	*AKAP8*	1.06
123	P35637	RNA-binding protein FUS	*FUS*	1.06
124	H3BQF1	Adenine phosphoribosyltransferase	*APRT*	1.06
125	Q92598	Heat shock protein 105 kDa	*HSPH1*	1.06
126	P32119	Peroxiredoxin-2	*PRDX2*	1.06
127	P12277	Creatine kinase B-type	*CKB*	1.06
128	E7ES10	Calpastatin	*CAST*	1.06
129	P35520	Cystathionine β-synthase	*CBS*	1.06
130	Q9UL46	Proteasome activator complex subunit 2	*PSME2*	1.06
131	P42704	Leucine-rich PPR motif-containing protein, mitochondrial	*LRPPRC*	1.06
132	E9PRQ7	UBX domain-containing protein 1	*UBXN1*	1.06
133	K7EL02	Thimet oligopeptidase	*THOP1*	1.06
134	Q32Q12	Nucleoside diphosphate kinase	*NME1-NME2*	1.06
135	Q07666	KH domain-containing, RNA-binding, signal transduction-associated protein 1	*KHDRBS1*	1.06
136	P04843	Dolichyl-diphosphooligosaccharide-protein glycosyltransferase subunit 1	*RPN1*	1.06
137	P49588	Alanine-tRNA ligase, cytoplasmic	*AARS*	1.06
138	O75367	Core histone macro-H2A.1	*H2AFY*	1.06
139	F8VZ29	Ubiquitin-conjugating enzyme E2 N	*UBE2N*	1.05
140	Q9P258	Protein RCC2	*RCC2*	1.60
141	P30101	Protein disulfide-isomerase A3	*PDIA3*	1.05
142	Q9BWD1	Acetyl-CoA acetyltransferase, cytosolic	*ACAT2*	1.05
143	P13797	Plastin-3	*PLS3*	1.05
144	P27824	Calnexin	*CANX*	1.05
145	P07900	Heat shock protein HSP 90-α	*HSP90AA1*	1.05
146	P04792	Heat shock protein β-1	*HSPB1*	1.05
147	P09972	Fructose-bisphosphate aldolase C	*ALDOC*	1.05
148	Q16658	Fascin	*FSCN1*	1.05
149	P07602	Proactivator polypeptide	*PSAP*	1.05
150	A6NKB8	Aminopeptidase B	*RNPEP*	1.05
151	P53396	ATP-citrate synthase	*ACLY*	1.05
152	H7BZJ3	Thioredoxin	*PDIA3*	1.05
153	B4DJV2	Citrate synthase	*CS*	1.04
154	Q12906	Interleukin enhancer-binding factor 3	*ILF3*	1.04
155	P09874	Poly [ADP-ribose] polymerase 1	*PARP1*	1.04
156	P13667	Protein disulfide-isomerase A4	*PDIA4*	1.04
157	P22102	Trifunctional purine biosynthetic protein adenosine-3	*GART*	1.04
158	Q96I24	Far upstream element-binding protein 3	*FUBP3*	1.04
159	E9PF10	Nuclear pore complex protein Nup155	*NUP155*	1.04
160	Q99460	26S proteasome non-ATPase regulatory subunit 1	*PSMD1*	1.04
161	P45880	Voltage-dependent anion-selective channel protein 2	*VDAC2*	1.04
162	Q13263	Transcription intermediary factor 1-β	*TRIM28*	1.04
163	O95373	Importin-7	*IPO7*	1.04
164	O95573	Long-chain-fatty-acid--CoA ligase 3	*ACSL3*	1.04
165	Q15084	Protein disulfide-isomerase A6	*PDIA6*	1.04
166	P62805	Histone H4	*HIST1H4A*	1.04
167	O60664	Perilipin-3	*PLIN3*	1.04
168	P26599	Polypyrimidine tract-binding protein 1	*PTBP1*	1.04

169	P17844	Probable ATP-dependent RNA helicase DDX5	*DDX5*	1.04
170	Q15393	Splicing factor 3B subunit 3	*SF3B3*	1.04
171	P38646	Stress-70 protein, mitochondrial	*HSPA9*	1.04
172	P50395	Rab GDP dissociation inhibitor beta	*GDI2*	1.04
173	Q04917	14-3-3 protein η	*YWHAH*	1.04
174	P54727	UV excision repair protein RAD23 homolog B	*RAD23B*	1.04
175	P35580	Myosin-10	*MYH10*	1.04
176	P68363	Tubulin alpha-1B chain	*TUBA1B*	1.04
177	P07108	Acyl-CoA-binding protein	*DBI*	1.04
178	Q15185	Prostaglandin E synthase 3	*PTGES3*	1.04
179	P49327	Fatty acid synthase	*FASN*	1.03
180	Q16777	Histone H2A type 2-C	*HIST2H2AC*	1.03
181	Q9BSJ8	Extended synaptotagmin-1	*ESYT1*	1.03
182	P00441	Superoxide dismutase [Cu-Zn]	*SOD1*	1.03
183	Q15365	Poly(rC)-binding protein 1	*PCBP1*	1.03
184	P47897	Glutamine-tRNA ligase	*QARS*	1.03
185	Q8TAT6	Nuclear protein localization protein 4 homolog	*NPLOC4*	1.03
186	A8MXP8	Reticulocalbin-2	*RCN2*	1.03
187	P07237	Protein disulfide-isomerase	*P4HB*	1.03
188	P45974	Ubiquitin carboxyl-terminal hydrolase 5	*USP5*	1.03
189	P50502	Hsc70-interacting protein	*ST13*	1.03
190	O75643	U5 small nuclear ribonucleoprotein 200 kDa helicase	*SNRNP200*	1.03
191	Q92499	ATP-dependent RNA helicase DDX1	*DDX1*	1.03
192	Q8WUM4	Programmed cell death 6-interacting protein	*PDCD6IP*	1.03
193	Q12874	Splicing factor 3A subunit 3	*SF3A3*	1.03
194	E7EX73	Eukaryotic translation initiation factor 4 γ1	*EIF4G1*	1.03
195	P11142	Heat shock cognate 71 kDa protein	*HSPA8*	1.03
196	Q15233	Non-POU domain-containing octamer-binding protein	*NONO*	1.03
197	Q9NY33	Dipeptidyl peptidase 3	*DPP3*	1.03
198	E9PMH2	Peptidyl-prolyl *cis-trans* isomerase	*AIP*	1.03
199	Q92973	Transportin-1	*TNPO1*	1.03
200	Q01081	Splicing factor U2AF 35 kDa subunit	*U2AF1*	1.03
201	Q14697	Neutral alpha-glucosidase AB	*GANAB*	1.03
202	Q9UHD8	Septin-9	9-Sep	1.03
203	K7EK07	Histone H3	*H3F3B*	1.03
204	Q15274	Nicotinate-nucleotide pyrophosphorylase [carboxylating]	*QPRT*	1.03
205	K7EJ57	Mitochondrial import receptor subunit TOM40 homolog	*TOMM40*	1.03
206	P28838	Cytosol aminopeptidase	*LAP3*	1.03
207	P62241	40S ribosomal protein S8	*RPS8*	1.03
208	P52272	Heterogeneous nuclear ribonucleoprotein M	*HNRNPM*	1.02
209	Q9BY32	Inosine triphosphate pyrophosphatase	*ITPA*	1.02
210	Q9HB71	Calcyclin-binding protein	*CACYBP*	1.02
211	Q92841	Probable ATP-dependent RNA helicase DDX17	*DDX17*	1.02
212	Q06210	Glutamine-fructose-6-phosphate aminotransferase [isomerizing] 1	*GFPT1*	1.02
213	Q92945	Far upstream element-binding protein 2	*KHSRP*	1.02
214	Q9BTT0	Acidic leucine-rich nuclear phosphoprotein 32 family member E	*ANP32E*	1.02
215	P46783	40S ribosomal protein S10	*RPS10*	1.02
216	O60701	UDP-glucose 6-dehydrogenase	*UGDH*	1.02
217	Q16643	Drebrin	*DBN1*	1.02
218	P68036	Ubiquitin-conjugating enzyme E2 L3	*UBE2L3*	1.02
219	P07384	Calpain-1 catalytic subunit	*CAPN1*	1.02
220	Q86VP6	Cullin-associated NEDD8-dissociated protein 1	*CAND1*	1.02
221	Q5JP53	Tubulin β chain	*TUBB*	1.02
222	O00410	Importin-5	*IPO5*	1.02
223	P35232	Prohibitin	*PHB*	1.02
224	P25705	ATP synthase subunit a, mitochondrial	*ATP5A1*	1.02
225	P04075	Fructose-bisphosphate aldolase A	*ALDOA*	1.02

226	P17174	Aspartate aminotransferase, cytoplasmic	*GOT1*	1.02
227	P61978	Heterogeneous nuclear ribonucleoprotein K	*HNRNPK*	1.02
228	K7EJE8	Lon protease homolog, mitochondrial	*LONP1*	1.02
229	Q04760	Lactoylglutathione lyase	*GLO1*	1.02
230	P68133	Actin, α skeletal muscle	*ACTA1*	1.01
231	Q99880	Histone H2B type 1-L	*HIST1H2BL*	1.01
232	B1ALC0	Actin-related protein 2/3 complex subunit 5	*ARPC5*	1.01
233	P78371	T-complex protein 1 subunit β	*CCT2*	1.01
234	P39748	Flap endonuclease 1	*FEN1*	1.01
235	O60506	Heterogeneous nuclear ribonucleoprotein Q	*SYNCRIP*	1.01
236	Q6XQN6	Nicotinate phosphoribosyltransferase	*NAPRT1*	1.01
237	P31946	14-3-3 protein β/α	*YWHAB*	1.01
238	P00387	NADH-cytochrome b_5 reductase 3	*CYB5R3*	1.01
239	P62258	14-3-3 protein ε	*YWHAE*	1.01
240	P10809	60 kDa heat shock protein, mitochondrial	*HSPD1*	1.01
241	P42166	Lamina-associated polypeptide 2, isoform α	*TMPO*	1.01
242	O75947	ATP synthase subunit d, mitochondrial	*ATP5H*	1.01
243	Q14444	Caprin-1	*CAPRIN1*	1.01
244	P26639	Threonine-tRNA ligase, cytoplasmic	*TARS*	1.01
245	P55072	Transitional endoplasmic reticulum ATPase	*VCP*	1.01
246	P67809	Nuclease-sensitive element-binding protein 1	*YBX1*	1.01
247	B7Z972	Protein-L-isoaspartate *O*-methyltransferase	*PCMT1*	1.01
248	B1AK85	F-actin-capping protein subunit β	*CAPZB*	1.01
249	Q13838	Spliceosome RNA helicase DDX39B	*DDX39B*	1.01
250	P08758	Annexin A5	*ANXA5*	1.01
251	O43707	α-Actinin-4	*ACTN4*	1.01
252	P06576	ATP synthase subunit β, mitochondrial	*ATP5B*	1.01
253	P30740	Leukocyte elastase inhibitor	*SERPINB1*	1.01
254	P62424	60S ribosomal protein L7a	*RPL7A*	1.01
255	O60832	H/ACA ribonucleoprotein complex subunit 4	*DKC1*	1.01
256	F8VZX2	Poly(rC)-binding protein 2	*PCBP2*	1.01
257	F8W1N5	Nascent polypeptide-associated complex subunit α	*NACA*	1.00
258	Q9UKY7	Protein CDV3 homolog	*CDV3*	1.00
259	P14866	Heterogeneous nuclear ribonucleoprotein L	*HNRNPL*	1.00
260	P06733	α-Enolase	*ENO1*	1.00
261	P62979	Ubiquitin-40S ribosomal protein S27a	*RPS27A*	1.00
262	F8WJN3	Cleavage and polyadenylation specificity factor subunit 6	*CPSF6*	1.00
263	P43686	26S protease regulatory subunit 6B	*PSMC4*	1.00
264	B4DQU5	Ras-related protein Rab-11A	*RAB11A*	1.00
265	O43143	Putative pre-mRNA-splicing factor ATP-dependent RNA helicase DHX15	*DHX15*	1.00
266	Q13813	Spectrin α chain, non-erythrocytic 1	*SPTAN1*	1.00
267	P68431	Histone H3.1	*HIST1H3A*	1.00
268	Q9Y624	Junctional adhesion molecule A	*F11R*	1.00
269	P26640	Valine-tRNA ligase	*VARS*	1.00
270	Q9NTK5	Obg-like ATPase 1	*OLA1*	1.00
271	P30086	Phosphatidylethanolamine-binding protein 1	*PEBP1*	1.00
272	E9PM92	Small acidic protein	*C11orf58*	1.00
273	H0Y8E6	DNA replication licensing factor MCM2	*MCM2*	1.00
274	F8VVM2	Phosphate carrier protein, mitochondrial	*SLC25A3*	1.00
275	P21333	Filamin-A	*FLNA*	1.00
276	P61158	Actin-related protein 3	*ACTR3*	1.00
277	P46060	Ran GTPase-activating protein 1	*RANGAP1*	1.00
278	Q9Y265	RuvB-like 1	*RUVBL1*	1.00
279	Q00839	Heterogeneous nuclear ribonucleoprotein U	*HNRNPU*	1.00
280	P63241	Eukaryotic translation initiation factor 5A-1	*EIF5A*	1.00
281	Q01105	Protein SET	*SET*	1.00
282	P60842	Eukaryotic initiation factor 4A-I	*EIF4A1*	1.00

283	Q86UY0	Thioredoxin domain-containing protein 5	*TXNDC5*	1.00
284	A6PVN8	Serine/threonine-protein phosphatase 2A activator	*PPP2R4*	1.00
285	F8VY35	Nucleosome assembly protein 1-like 1	*NAP1L1*	1.00
286	P52209	6-Phosphogluconate dehydrogenase, decarboxylating	*PGD*	1.00
287	F8VWS0	60S acidic ribosomal protein P0	*RPLP0*	1.00
288	H0YFA4	Cysteine-rich protein 2	*CRIP2*	1.00
289	Q16555	Dihydropyrimidinase-related protein 2	*DPYSL2*	1.00
290	P02545	Prelamin-A/C	*LMNA*	1.00
291	P07737	Profilin-1	*PFN1*	1.00
292	O60488	Long-chain-fatty-acid--CoA ligase 4	*ACSL4*	1.00
293	P61160	Actin-related protein 2	*ACTR2*	0.99
294	P43243	Matrin-3	*MATR3*	0.99
295	Q96P70	Importin-9	*IPO9*	0.99
296	P13010	X-ray repair cross-complementing protein 5	*XRCC5*	0.99
297	P27348	14-3-3 protein θ	*YWHAQ*	0.99
298	F8W7C6		RPL10	0.99
299	Q9ULV4	Coronin-1C	*CORO1C*	0.99
300	Q3ZCM7	Tubulin β-8 chain	*TUBB8*	0.99
301	Q6DKJ4	Nucleoredoxin	*NXN*	0.99
302	O14579	Coatomer subunit ε	*COPE*	0.99
303	P00352	Retinal dehydrogenase 1	*ALDH1A1*	0.99
304	P61981	14-3-3 protein γ	*YWHAG*	0.99
305	K7ELL7	Glucosidase 2 subunit β	*PRKCSH*	0.99
306	P63104	14-3-3 protein ζ/δ	*YWHAZ*	0.99
307	P62937	Peptidyl-prolyl *cis-trans* isomerase A	*PPIA*	0.99
308	Q71DI3	Histone H3.2	*HIST2H3A*	0.99
309	Q13185	Chromobox protein homolog 3	*CBX3*	0.99
310	Q9NR30	Nucleolar RNA helicase 2	*DDX21*	0.99
311	Q99714	3-Hydroxyacyl-CoA dehydrogenase type-2	*HSD17B10*	0.99
312	Q8NC51	Plasminogen activator inhibitor 1 RNA-binding protein	*SERBP1*	0.99
313	B7Z7P8	Eukaryotic peptide chain release factor subunit 1	*ETF1*	0.99
314	Q13347	Eukaryotic translation initiation factor 3 subunit I	*EIF3I*	0.99
315	Q9Y490	Talin-1	*TLN1*	0.99
316	P63261	Actin, cytoplasmic 2	*ACTG1*	0.99
317	P62314	Small nuclear ribonucleoprotein Sm D1	*SNRPD1*	0.99
318	P49411	Elongation factor Tu, mitochondrial	*TUFM*	0.99
319	P12956	X-ray repair cross-complementing protein 6	*XRCC6*	0.99
320	P07858	Cathepsin B	*CTSB*	0.99
321	P12004	Proliferating cell nuclear antigen	*PCNA*	0.99
322	P35221	Catenin α-1	*CTNNA1*	0.99
323	Q99733	Nucleosome assembly protein 1-like 4	*NAP1L4*	0.98
324	P62633	Cellular nucleic acid-binding protein	*CNBP*	0.98
325	Q92575	UBX domain-containing protein 4	*UBXN4*	0.98
326	Q06830	Peroxiredoxin-1	*PRDX1*	0.98
327	P40227	T-complex protein 1 subunit θ	*CCT6A*	0.98
328	Q9NS69	Mitochondrial import receptor subunit TOM22 homolog	*TOMM22*	0.98
329	H7C469	Cathepsin D	*CTSD*	0.98
330	P31939	Bifunctional purine biosynthesis protein PURH	*ATIC*	0.98
331	Q7KZF4	Staphylococcal nuclease domain-containing protein 1	*SND1*	0.98
332	H0YK49	Electron transfer flavoprotein subunit α, mitochondrial	*ETFA*	0.98
333	P18669	Phosphoglycerate mutase 1	*PGAM1*	0.98
334	Q00610	Clathrin heavy chain 1	*CLTC*	0.98
335	P40926	Malate dehydrogenase, mitochondrial	*MDH2*	0.98
336	P40925	Malate dehydrogenase, cytoplasmic	*MDH1*	0.98
337	E9PBS1	Multifunctional protein ADE2	*PAICS*	0.98
338	P05386	60S acidic ribosomal protein P1	*RPLP1*	0.98
339	P04406	Glyceraldehyde-3-phosphate dehydrogenase	*GAPDH*	0.98

340	P23526	Adenosylhomocysteinase	*AHCY*	0.98
341	P50990	T-complex protein 1 subunit θ	*CCT8*	0.98
342	P49748	Very long-chain specific acyl-CoA dehydrogenase, mitochondrial	*ACADVL*	0.98
343	P46778	60S ribosomal protein L21	*RPL21*	0.98
344	P31942	Heterogeneous nuclear ribonucleoprotein H3	*HNRNPH3*	0.98
345	C9J9W2	LIM and SH3 domain protein 1	*LASP1*	0.98
346	Q92616	Translational activator GCN1	*GCN1L1*	0.98
347	Q9C005	Protein dpy-30 homolog	*DPY30*	0.98
348	P46109	Crk-like protein	*CRKL*	0.97
349	P27695	DNA-(apurinic or apyrimidinic site) lyase	*APEX1*	0.97
350	Q15181	Inorganic pyrophosphatase	*PPA1*	0.97
351	P62906	60S ribosomal protein L10a	*RPL10A*	0.97
352	O00299	Chloride intracellular channel protein 1	*CLIC1*	0.97
353	E7EMC7	Sequestosome-1	*SQSTM1*	0.97
354	P49257	Protein ERGIC-53	*LMAN1*	0.97
355	P36578	60S ribosomal protein L4	*RPL4*	0.97
356	P63010	AP-2 complex subunit β	*AP2B1*	0.97
357	P62263	40S ribosomal protein S14	*RPS14*	0.97
358	P04632	Calpain small subunit 1	*CAPNS1*	0.97
359	B4DUR8	T-complex protein 1 subunit γ	*CCT3*	0.97
360	Q99613	Eukaryotic translation initiation factor 3 subunit C	*EIF3C*	0.97
361	E9PPJ0	Splicing factor 3B subunit 2	*SF3B2*	0.97
362	Q9BVA1	Tubulin β-2B chain	*TUBB2B*	0.97
363	P27797	Calreticulin	*CALR*	0.97
364	Q14204	Cytoplasmic dynein 1 heavy chain 1	*DYNC1H1*	0.97
365	Q08945	FACT complex subunit SSRP1	*SSRP1*	0.97
366	P23528	Cofilin-1	*CFL1*	0.97
367	P06744	Glucose-6-phosphate isomerase	*GPI*	0.97
368	O00425	Insulin-like growth factor 2 mRNA-binding protein 3	*IGF2BP3*	0.97
369	P56192	Methionine-tRNA ligase, cytoplasmic	*MARS*	0.97
370	P60174	Triosephosphate isomerase	*TPI1*	0.97
371	P26641	Elongation factor 1-γ	*EEF1G*	0.97
372	C9JJ34	Ran-specific GTPase-activating protein	*RANBP1*	0.96
373	Q5VU59	-	*TPM3*	0.96
374	P55884	Eukaryotic translation initiation factor 3 subunit B	*EIF3B*	0.96
375	P00558	Phosphoglycerate kinase 1	*PGK1*	0.96
376	E5RI99	60S ribosomal protein L30	*RPL30*	0.96
377	P06748	Nucleophosmin	*NPM1*	0.96
378	P20042	Eukaryotic translation initiation factor 2 subunit 2	*EIF2S2*	0.96
379	P00367	Glutamate dehydrogenase 1, mitochondrial	*GLUD1*	0.96
380	P20700	Lamin-B1	*LMNB1*	0.96
381	P08727	Keratin, type I cytoskeletal 19	*KRT19*	0.96
382	Q08211	ATP-dependent RNA helicase A	*DHX9*	0.96
383	P42224	Signal transducer and activator of transcription 1-α/β	*STAT1*	0.96
384	O75369	Filamin-B	*FLNB*	0.96
385	O75083	WD repeat-containing protein 1	*WDR1*	0.96
386	Q15056	Eukaryotic translation initiation factor 4H	*EIF4H*	0.96
387	J3KPE3	Guanine nucleotide-binding protein subunit β-2-like 1	*GNB2L1*	0.96
388	Q8WXF1	Paraspeckle component 1	*PSPC1*	0.96
389	P05387	60S acidic ribosomal protein P2	*RPLP2*	0.96
390	P41250	Glycine-tRNA ligase	*GARS*	0.96
391	P14324	Farnesyl pyrophosphate synthase	*FDPS*	0.96
392	P30153	Serine/threonine-protein phosphatase 2A 65 kDa regulatory subunit Aα isoform	*PPP2R1A*	0.96
393	P14618	Pyruvate kinase PKM	*PKM*	0.96
394	P35268	60S ribosomal protein L22	*RPL22*	0.96
395	Q8N8S7	Protein enabled homolog	*ENAH*	0.96
396	P53621	Coatomer subunit α	*COPA*	0.96

397	E7EQR4	Ezrin	*EZR*	0.95
398	F8VPF3	Myosin light polypeptide 6	*MYL6*	0.95
399	C9J9K3	40S ribosomal protein SA	*RPSA*	0.95
400	Q99497	Protein DJ-1	*PARK7*	0.95
401	Q00341	Vigilin	*HDLBP*	0.95
402	P18124	60S ribosomal protein L7	*RPL7*	0.95
403	P20290	Transcription factor BTF3	*BTF3*	0.95
404	Q10567	AP-1 complex subunit β-1	*AP1B1*	0.95
405	H0YEN5	40S ribosomal protein S2	*RPS2*	0.95
406	P00338	L-lactate dehydrogenase A chain	*LDHA*	0.95
407	P38919	Eukaryotic initiation factor 4A-III	*EIF4A3*	0.95
408	P55060	Exportin-2	*CSE1L*	0.95
409	P53618	Coatomer subunit β	*COPB1*	0.95
410	P50991	T-complex protein 1 subunit δ	*CCT4*	0.95
411	P24534	Elongation factor 1-β	*EEF1B2*	0.95
412	P07355	Annexin A2	*ANXA2*	0.95
413	Q9UNZ2	NSFL1 cofactor p47	*NSFL1C*	0.95
414	P30041	Peroxiredoxin-6	*PRDX6*	0.95
415	O95433	Activator of 90 kDa heat shock protein ATPase homolog 1	*AHSA1*	0.94
416	H3BND8	Ubiquitin carboxyl-terminal hydrolase	*USP7*	0.94
417	P62136	Serine/threonine-protein phosphatase PP1-α catalytic subunit	*PPP1CA*	0.94
418	P12814	α-Actinin-1	*ACTN1*	0.94
419	P37802	Transgelin-2	*TAGLN2*	0.94
420	P51654	Glypican-3	*GPC3*	0.94
421	Q9UMS4	Pre-mRNA-processing factor 19	*PRPF19*	0.94
422	P25398	40S ribosomal protein S12	*RPS12*	0.94
423	P51991	Heterogeneous nuclear ribonucleoprotein A3	*HNRNPA3*	0.94
424	E7EQV3	Polyadenylate-binding protein 1	*PABPC1*	0.94
425	P61353	60S ribosomal protein L27	*RPL27*	0.94
426	B4E022	Transketolase	*TKT*	0.94
427	P13639	Elongation factor 2	*EEF2*	0.94
428	P22087	rRNA 2-O-methyltransferase fibrillarin	*FBL*	0.94
429	P39023	60S ribosomal protein L3	*RPL3*	0.93
430	Q9BR76	Coronin-1B	*CORO1B*	0.93
431	P46940	Ras GTPase-activating-like protein IQGAP1	*IQGAP1*	0.93
432	P26368	Splicing factor U2AF 65 kDa subunit	*U2AF2*	0.93
433	P30085	UMP-CMP kinase	*CMPK1*	0.93
434	O00629	Importin subunit α-3	*KPNA4*	0.93
435	Q13409	Cytoplasmic dynein 1 intermediate chain 2	*DYNC1I2*	0.93
436	Q14247	Src substrate cortactin	*CTTN*	0.93
437	P46379	Large proline-rich protein BAG6	*BAG6*	0.93
438	E9PLD0	Ras-related protein Rab-1B	*RAB1B*	0.93
439	P78344	Eukaryotic translation initiation factor 4 γ 2	*EIF4G2*	0.93
440	P29692	Elongation factor 1-δ	*EEF1D*	0.93
441	A6NHL2	Tubulin alpha chain-like 3	*TUBAL3*	0.93
442	P32969	60S ribosomal protein L9	*RPL9*	0.93
443	P25786	Proteasome subunit alpha type-1	*PSMA1*	0.93
444	Q07021	Complement component 1 Q subcomponent-binding protein, mitochondrial	*C1QBP*	0.93
445	Q01082	Spectrin beta chain, non-erythrocytic 1	*SPTBN1*	0.93
446	Q01518	Adenylyl cyclase-associated protein 1	*CAP1*	0.93
447	P78347	General transcription factor II-I	*GTF2I*	0.93
448	F5GY37	Prohibitin-2	*PHB2*	0.92
449	P08670	Vimentin	*VIM*	0.92
450	P68104	Elongation factor 1-α 1	*EEF1A1*	0.92
451	Q14315	Filamin-C	*FLNC*	0.92
452	P05787	Keratin, type II cytoskeletal 8	*KRT8*	0.92
453	O75533	Splicing factor 3B subunit 1	*SF3B1*	0.92

454	P13489	Ribonuclease inhibitor	*RNH1*	0.92
455	P05783	Keratin, type I cytoskeletal 18	*KRT18*	0.92
456	E7EUY0	DNA-dependent protein kinase catalytic subunit	*PRKDC*	0.92
457	J3KN67	Tropomyosin α-3 chain	*TPM3*	0.92
458	G3V1A1	60S ribosomal protein L8	*RPL8*	0.91
459	Q5T7C4	High mobility group protein B1	*HMGB1*	0.91
460	Q9Y281	Cofilin-2	*CFL2*	0.91
461	P09382	Galectin-1	*LGALS1*	0.91
462	Q9UQ80	Proliferation-associated protein 2G4	*PA2G4*	0.91
463	P09327	Villin-1	*VIL1*	0.91
464	Q6P2Q9	Pre-mRNA-processing-splicing factor 8	*PRPF8*	0.91
465	P26196	Probable ATP-dependent RNA helicase DDX6	*DDX6*	0.91
466	Q9NZI8	Insulin-like growth factor 2 mRNA-binding protein 1	*IGF2BP1*	0.91
467	P51858	Hepatoma-derived growth factor	*HDGF*	0.91
468	Q13126	S-methyl-5-thioadenosine phosphorylase	*MTAP*	0.91
469	Q9UHX1	Poly(U)-binding-splicing factor PUF60	*PUF60*	0.91
470	Q12904	Aminoacyl tRNA synthase complex-interacting multifunctional protein 1	*AIMP1*	0.90
471	P02786	Transferrin receptor protein 1	*TFRC*	0.90
472	P14868	Aspartate-tRNA ligase, cytoplasmic	*DARS*	0.90
473	C9JD32	60S ribosomal protein L23	*RPL23*	0.90
474	Q15149	Plectin	*PLEC*	0.90
475	Q14566	DNA replication licensing factor MCM6	*MCM6*	0.90
476	P49915	GMP synthase [glutamine-hydrolyzing]	*GMPS*	0.90
477	H0Y4R1	Inosine-5-monophosphate dehydrogenase 2	*IMPDH2*	0.90
478	F8VUA6	60S ribosomal protein L18	*RPL18*	0.90
479	Q15942	Zyxin	*ZYX*	0.90
480	O00151	PDZ and LIM domain protein 1	*PDLIM1*	0.90
481	P30050	60S ribosomal protein L12	*RPL12*	0.90
482	P30048	Thioredoxin-dependent peroxide reductase, mitochondrial	*PRDX3*	0.90
483	P16422	Epithelial cell adhesion molecule	*EPCAM*	0.90
484	J3KTF8	Rho GDP-dissociation inhibitor 1	*ARHGDIA*	0.90
485	P18206	Vinculin	*VCL*	0.89
486	O14979	Heterogeneous nuclear ribonucleoprotein D-like	*HNRPDL*	0.89
487	M0QZS6	SUMO-activating enzyme subunit 1	*SAE1*	0.89
488	P29966	Myristoylated alanine-rich C-kinase substrate	*MARCKS*	0.89
489	P04040	Catalase	*CAT*	0.89
490	H0YE29	Rho GTPase-activating protein 1	*ARHGAP1*	0.89
491	Q96AG4	Leucine-rich repeat-containing protein 59	*LRRC59*	0.89
492	Q02790	Peptidyl-prolyl *cis-trans* isomerase FKBP4	*FKBP4*	0.89
493	P02768	Serum albumin	*ALB*	0.89
494	Q16531	DNA damage-binding protein 1	*DDB1*	0.89
495	B7Z7F3	Ran-binding protein 3	*RANBP3*	0.89
496	P40429	60S ribosomal protein L13a	*RPL13A*	0.89
497	K7ERT7	Synaptic vesicle membrane protein VAT-1 homolog	*VAT1*	0.88
498	Q13907	Isopentenyl-diphosphate δ-isomerase 1	*IDI1*	0.88
499	O43852	Calumenin	*CALU*	0.88
500	Q13162	Peroxiredoxin-4	*PRDX4*	0.88
501	D6R938	Calcium/calmodulin-dependent protein kinase type II subunit δ	*CAMK2D*	0.88
502	Q7L2H7	Eukaryotic translation initiation factor 3 subunit M	*EIF3M*	0.87
503	P84077	ADP-ribosylation factor 1	*ARF1*	0.87
504	P21796	Voltage-dependent anion-selective channel protein 1	*VDAC1*	0.87
505	P15924	Desmoplakin	*DSP*	0.87
506	P20618	Proteasome subunit β type-1	*PSMB1*	0.86
507	P25205	DNA replication licensing factor MCM3	*MCM3*	0.86
508	Q16836	Hydroxyacyl-coenzyme A dehydrogenase, mitochondrial	*HADH*	0.86
509	E7ETK0	40S ribosomal protein S24	*RPS24*	0.86
510	Q9NVJ2	ADP-ribosylation factor-like protein 8B	*ARL8B*	0.86

511	P12955	Xaa-Pro dipeptidase	*PEPD*	0.86
512	Q86V81	THO complex subunit 4	*ALYREF*	0.86
513	Q9BSE5	Agmatinase, mitochondrial	*AGMAT*	0.86
514	E7EPN9	Protein PRRC2C	*PRRC2C*	0.85
515	Q9Y333	U6 snRNA-associated Sm-like protein LSm2	*LSM2*	0.85
516	P50135	Histamine *N*-methyltransferase	*HNMT*	0.85
517	G3V119	DBIRD complex subunit KIAA1967	*KIAA1967*	0.85
518	Q9NQC3	Reticulon-4	*RTN4*	0.85
519	P40939	Trifunctional enzyme subunit α, mitochondrial	*HADHA*	0.85
520	P41252	Isoleucine-tRNA ligase, cytoplasmic	*IARS*	0.85
521	P58546	Myotrophin	*MTPN*	0.84
522	K7EJ78	40S ribosomal protein S15	*RPS15*	0.84
523	O75937	DnaJ homolog subfamily C member 8	*DNAJC8*	0.84
524	P25787	Proteasome subunit α type-2	*PSMA2*	0.84
525	Q8IV08	Phospholipase D3	*PLD3*	0.84
526	Q09666	Neuroblast differentiation-associated protein AHNAK	*AHNAK*	0.84
527	P21291	Cysteine and glycine-rich protein 1	*CSRP1*	0.84
528	P10768	*S*-formylglutathione hydrolase	*ESD*	0.83
529	Q96QK1	Vacuolar protein sorting-associated protein 35	*VPS35*	0.83
530	C9JDE9	3-Ketoacyl-CoA thiolase, peroxisomal	*ACAA1*	0.82
531	P17655	Calpain-2 catalytic subunit	*CAPN2*	0.82
532	P46777	60S ribosomal protein L5	*RPL5*	0.81
533	Q15424	Scaffold attachment factor B1	*SAFB*	0.81
534	Q9H6S3	Epidermal growth factor receptor kinase substrate 8-like protein 2	*EPS8L2*	0.81
535	Q96C90	Protein phosphatase 1 regulatory subunit 14B	*PPP1R14B*	0.80
536	Q9P0L0	Vesicle-associated membrane protein-associated protein A	*VAPA*	0.79
537	O43242	26S proteasome non-ATPase regulatory subunit 3	*PSMD3*	0.79
538	P00390	Glutathione reductase, mitochondrial	*GSR*	0.78
539	Q9Y678	Coatomer subunit γ-1	*COPG1*	0.78
540	P26038	Moesin	*MSN*	0.77
541	O96019	Actin-like protein 6A	*ACTL6A*	0.77
542	P05023	Sodium/potassium-transporting ATPase subunit α-1	*ATP1A1*	0.76
543	P62081	40S ribosomal protein S7	*RPS7*	0.76
544	D6RG13	40S ribosomal protein S3a	*RPS3A*	0.76
545	E9PIR7	Thioredoxin reductase 1, cytoplasmic	*TXNRD1*	0.76
546	Q9UBB4	Ataxin-10	*ATXN10*	0.75
547	P10644	cAMP-dependent protein kinase type I-α regulatory subunit	*PRKAR1A*	0.75
548	P11717	Cation-independent mannose-6-phosphate receptor	*IGF2R*	0.75
549	D6RG15	Twinfilin-2	*TWF2*	0.74
550	Q14152	Eukaryotic translation initiation factor 3 subunit A	*EIF3A*	0.74
551	P07954	Fumarate hydratase, mitochondrial	*FH*	0.73
552	Q9BXP5	Serrate RNA effector molecule homolog	*SRRT*	0.72
553	W4VSQ9	CDC42-interacting protein 4	*TRIP10*	0.72
554	P33991	DNA replication licensing factor MCM4	*MCM4*	0.70
555	P36542	ATP synthase subunit γ, mitochondrial	*ATP5C1*	0.69
556	P62701	40S ribosomal protein S4, X isoform	*RPS4X*	0.68
557	Q86TG7	Retrotransposon-derived protein PEG10	*PEG10*	0.66
558	Q16891	Mitochondrial inner membrane protein	*IMMT*	0.66
559	Q9UDY2	Tight junction protein ZO-2	*TJP2*	0.64
560	Q9NYL9	Tropomodulin-3	*TMOD3*	0.62
561	P02787	Serotransferrin	*TF*	0.59
562	B4DDF4	Calponin-2	*CNN2*	0.58
563	Q12792	Twinfilin-1	*TWF1*	0.49
564	Q16851	UTP-glucose-1-phosphate uridylyltransferase	*UGP2*	0.45
565	P04264	Keratin, type II cytoskeletal 1	*KRT1*	0.22
566	P35527	Keratin, type I cytoskeletal 9	*KRT9*	0.14

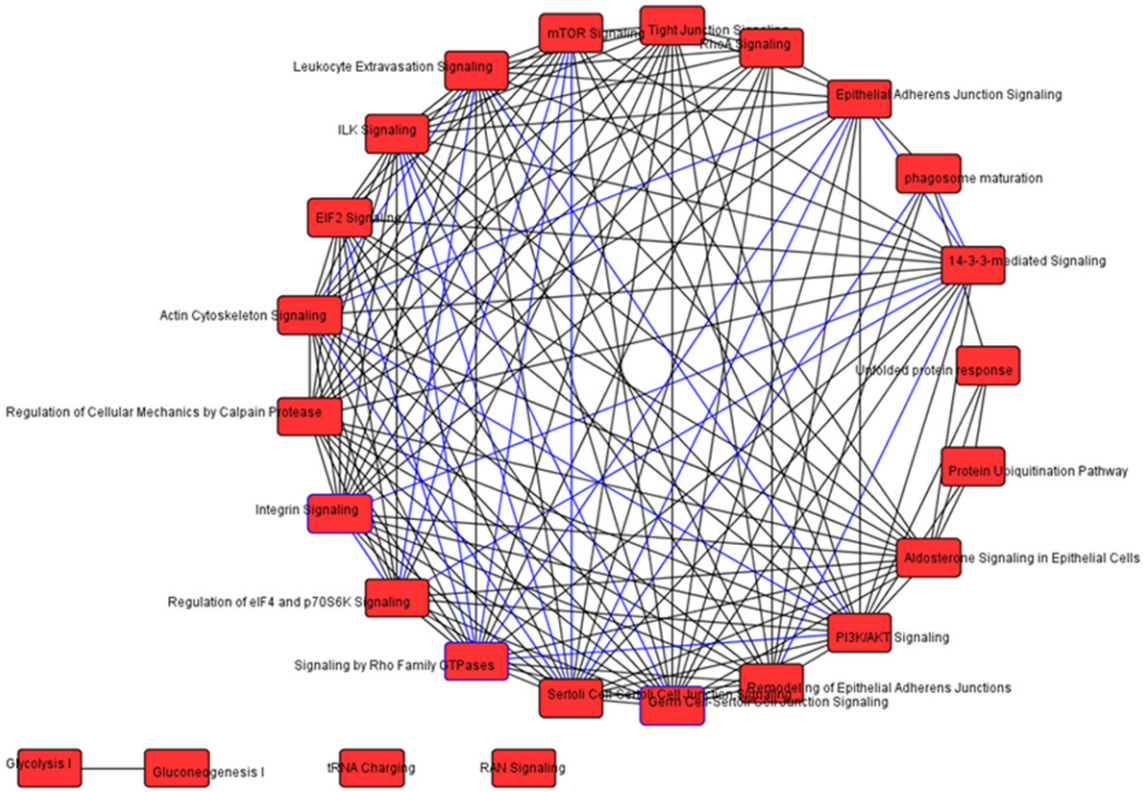

Figure S2. Proteomic analysis revealed 94 related pathways were regulated by ALS in Hep3B cells.

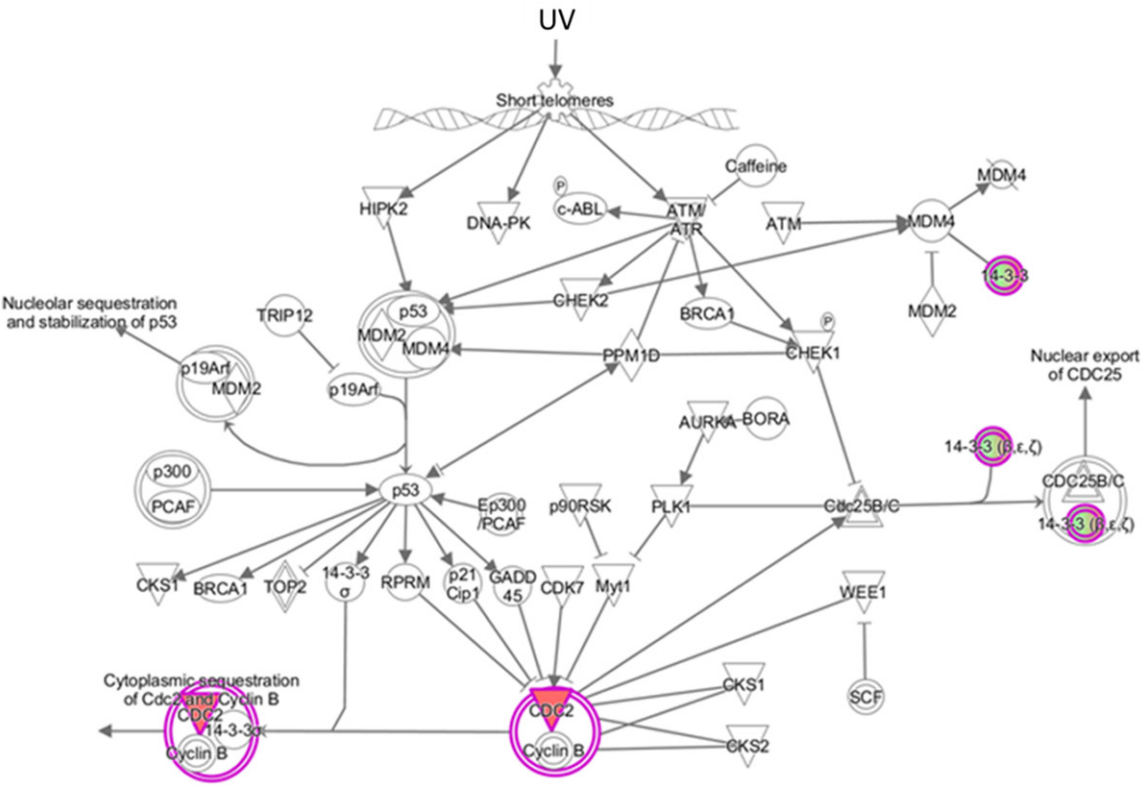

Figure S3. ALS regulates cell cycle at G_2/M checkpoint in Hep3B cells. Notes: Hep3B cells were treated with 1 μM ALS for 24 h and the protein samples were subject to quantitative proteomic analysis. Color indicates the molecules regulated by ALS.

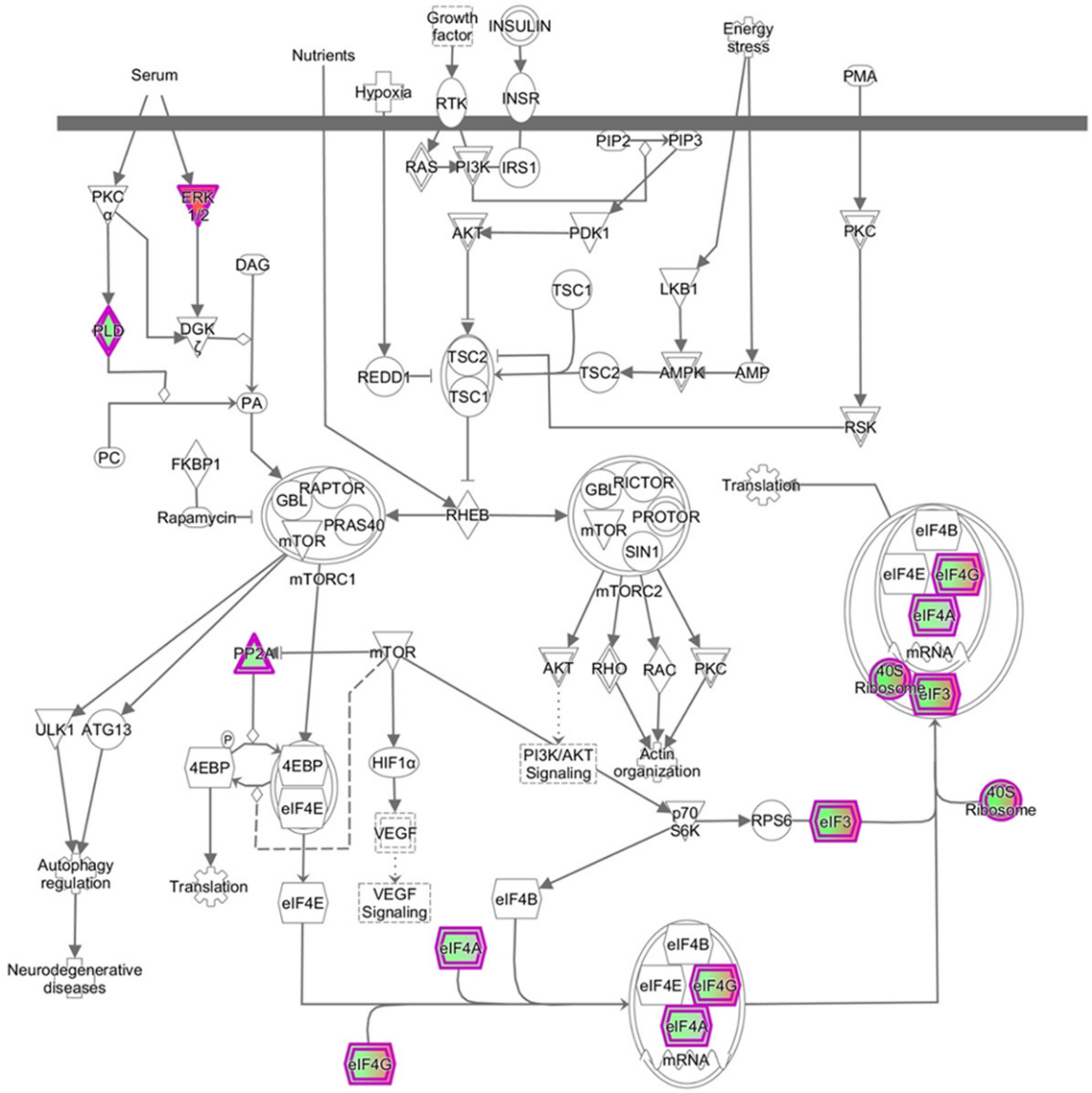

Figure S4. mTOR signaling pathway regulated by ALS in Hep3B cells. Notes: Hep3B cells were treated with 1 μM ALS for 24 h and the protein samples were subject to quantitative proteomic analysis. Color indicates the molecules regulated by ALS.

Table S2. The 94 Ingenuity Canonical Pathways regulated by alisertib in Hep3B cells (sorted by log *P* value)

No.	Ingenuity canonical pathways
1	EIF2 signaling
2	Regulation of eIF4 and p70S6K signaling
3	Remodeling of epithelial adherens junctions
4	RAN signaling
5	mTOR signaling
6	Protein ubiquitination pathway
7	Epithelial adherens junction signaling
8	tRNA charging
9	Glycolysis I
10	Gluconeogenesis I
11	Actin cytoskeleton signaling
12	14-3-3-mediated signaling
13	Unfolded protein response
14	ILK signaling
15	RhoA signaling
16	Regulation of cellular mechanics by calpain protease
17	Germ cell-Sertoli cell junction signaling
18	Sertoli cell-Sertoli cell junction signaling
19	Integrin signaling
20	Tight junction signaling
21	Aldosterone signaling in epithelial cells
22	PI3K/AKT signaling
23	Pyrimidine deoxyribonucleotides *de novo* biosynthesis I
24	Fatty Acid β-oxidation I
25	Clathrin-mediated endocytosis signaling
26	ERK/MAPK signaling
27	Mitochondrial dysfunction
28	HIPPO signaling
29	Caveolar-mediated endocytosis signaling
30	Signaling by Rho family GTPases
31	Leukocyte extravasation signaling
32	Cell Cycle: G_2/M DNA damage checkpoint regulation
33	Lipid antigen presentation by CD1
34	Protein kinase a signaling
35	Superpathway of geranygeranyldiphosphate biosynthesis (via mevalonate)
36	RhoGDI signaling
37	Superpathway of cholesterol biosynthesis
38	p70S6K signaling
39	NRF2-mediated oxidative stress response
40	Glutaryl-CoA degradation
41	Pentose phosphate pathway
42	VEGF signaling
43	BER pathway
44	Fcγ receptor-mediated phagocytosis in macrophages and monocytes
45	Breast cancer regulation by stathmin1
46	Mevalonate pathway I

47	TCA cycle
48	Gap junction signaling
49	DNA double-strand break repair by non-homologous end joining
50	Isoleucine degradation I
51	Telomere extension by telomerase
52	FAK signaling
53	Huntingtons disease signaling
54	Superpathway of serine and glycine biosynthesis I
55	Aspartate degradation II
56	Virus entry via endocytic pathways
57	Apoptosis signaling
58	Spliceosomal cycle
59	L-cysteine degradation III
60	Formaldehyde oxidation II (glutathione-dependent)
61	Granzyme B signaling
62	Mechanisms of viral exit from host cells
63	IGF-1 signaling
64	Sucrose degradation V (mammalian)
65	CDK5 signaling
66	Telomerase signaling
67	Tryptophan degradation X (mammalian, via tryptamine)
68	Hypoxia signaling in the cardiovascular system
69	Ketogenesis
70	Mitotic roles of Polo-like kinase
71	Inosine-5'-phosphate biosynthesis II
72	Regulation of actin-based motility by Rho
73	Ephrin B signaling
74	Myc mediated apoptosis signaling
75	Cell cycle control of chromosomal replication
76	Colanic acid building blocks biosynthesis
77	Paxillin signaling
78	Pentose phosphate pathway (oxidative branch)
79	Serine biosynthesis
80	Trans, *trans*-farnesyl diphosphate biosynthesis
81	Prostate cancer signaling
82	ERK5 signaling
83	Rac signaling
84	Pentose phosphate pathway (non-oxidative branch)
85	Superoxide radical degradation
86	γ-Linolenate biosynthesis II (animals)
87	PPARα/RXRα activation
88	Superpathway of methionine degradation
89	Cardiac β-adrenergic signaling
90	Ethanol degradation II
91	Ethanol degradation IV
92	Amyloid processing
93	Glucocorticoid receptor signaling
94	Cysteine biosynthesis III (mammalian)